SUPPLEMENTARY INFORMATION

Quinoline and Coumarin Isoxazole Derivatives: Synthesis, Antitumor Evaluation and Molecular Docking Studies with Bcl-2

Martina Piškor,[a] Marina Ter,[a] Leentje Persoons,[b] Dirk Daelemans,[b] Ahmed Adel,[c] Mutasem O. Taha,[d] Astrid Milić,[e] Mirela Sedić[f] and Silvana Raić-Malić[a*]

[a] Department of Organic Chemistry, Faculty of Chemical Engineering and Technology University of Zagreb, Marulićev trg 19, 10000 Zagreb, Croatia. E-mail: sraic@fkit.unizg.hr

[b] KU Leuven, Department of Microbiology, Immunology and Transplantation, Molecular Genetics and Therapeutics in Virology and Oncology Research Group, Rega Institute, 3000 Leuven, Belgium

[c] Faculty of pharmacy and Medical Sciences, University of Petra, Amman 11196, Jordan

[d] Department of Pharmaceutical Sciences, Faculty of Pharmacy, University of Jordan, Amman 11942, Jordan

[e] Selvita d.o.o., Zagreb 10000, Croatia

[f] Centre for Applied Bioanthropology, Institute for Anthropological Research, Zagreb, Croatia

Contents

1. ^{1}H and ^{13}C NMR spectra of novel compounds

1.1. ^{1}H and ^{13}C NMR spectra of quinoline (7a–e, 8a–f) and coumarin (9a–e) isoxazole derivatives

Figure S1: a) ^{1}H NMR and b) ^{13}C NMR of compd. **7a**.

a)

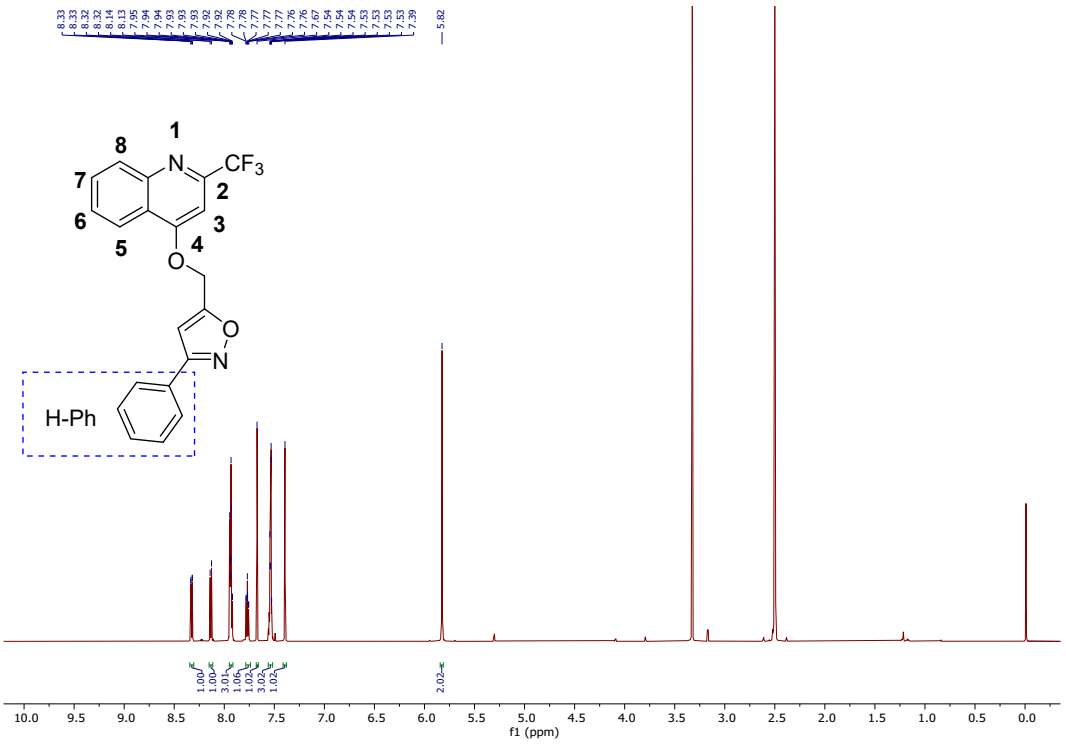

b)

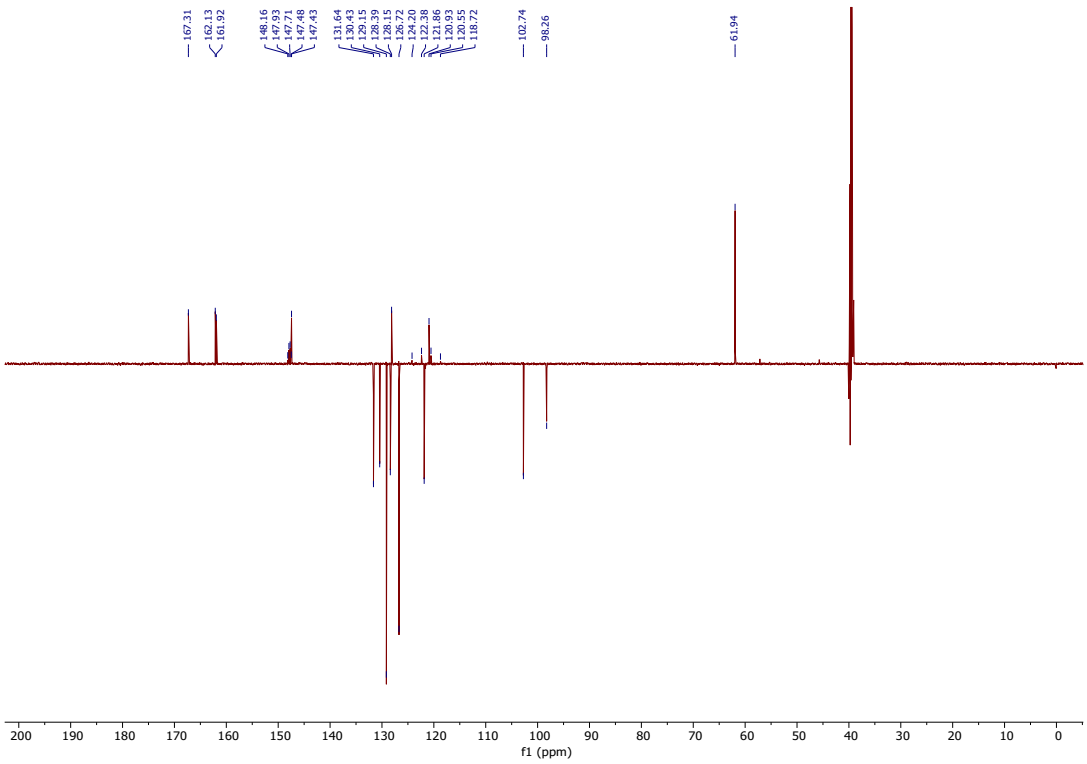

Figure S2: a) ^{1}H NMR and b) ^{13}C NMR c) COSY of compd. **7b** in DMSO-d_6.

a)

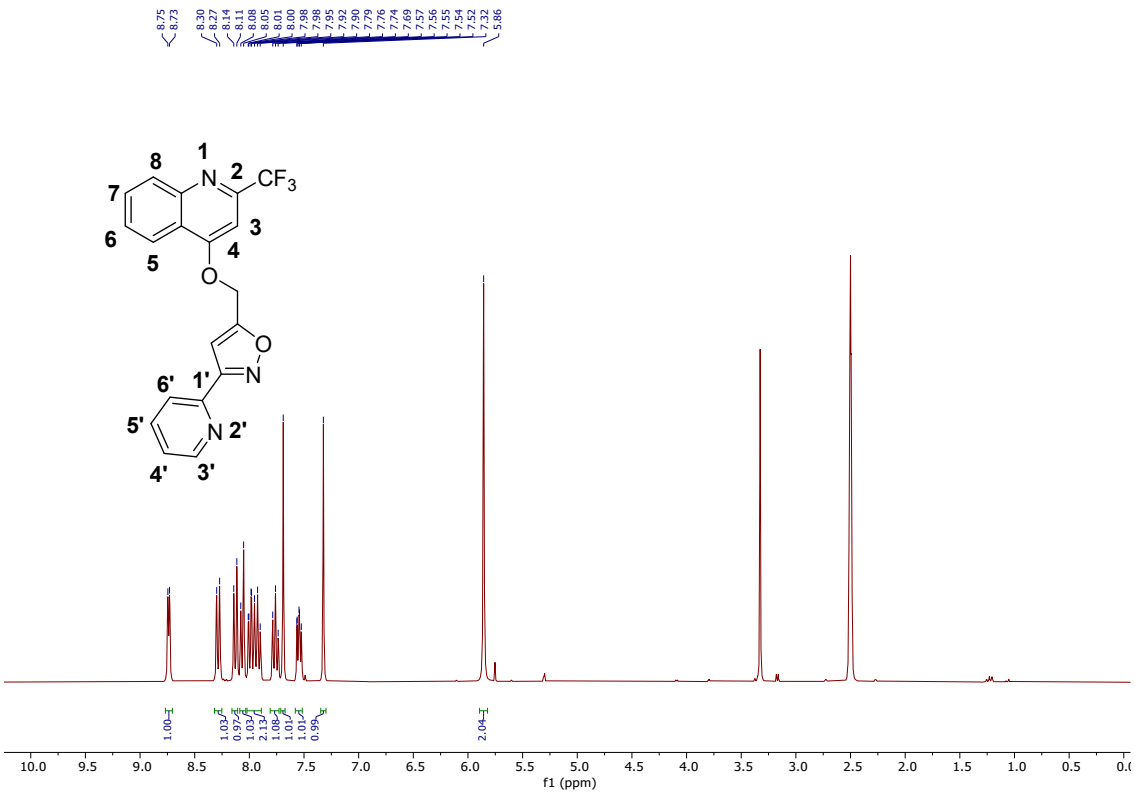

b)

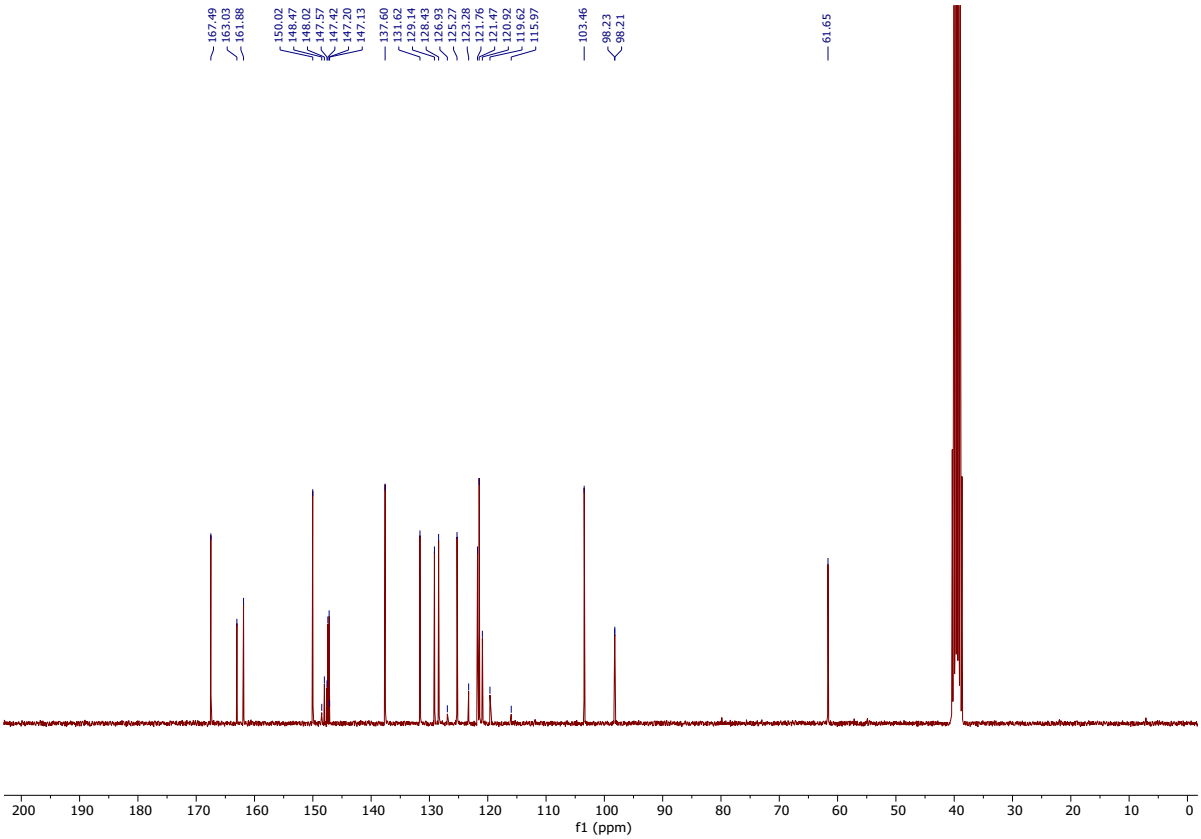

c)

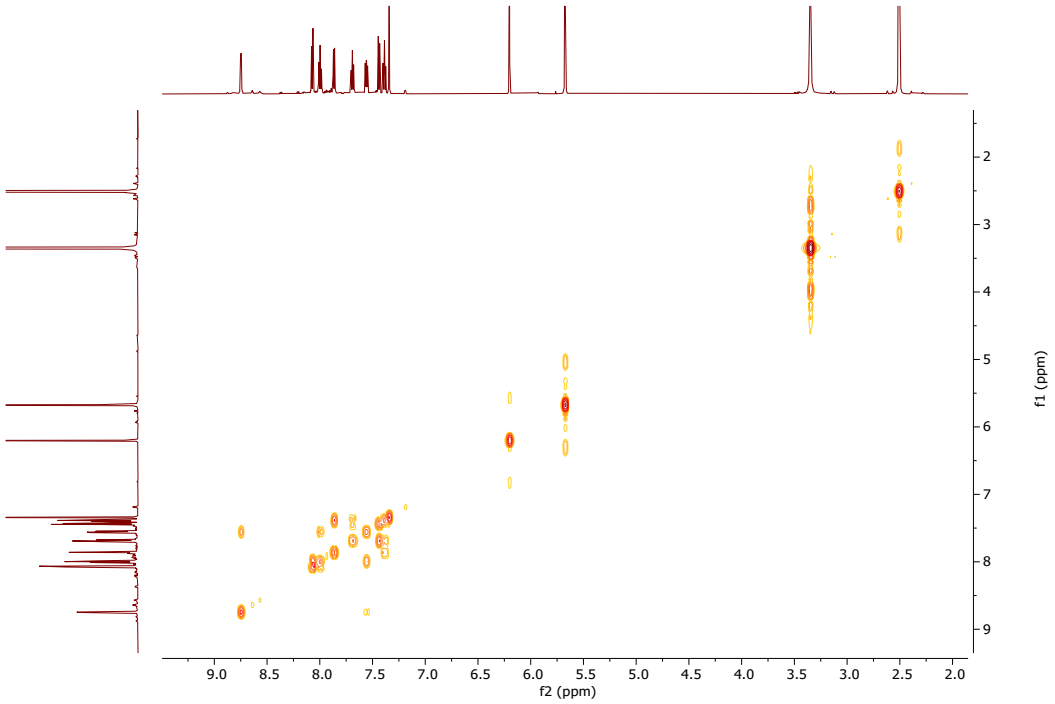

Figure S3: a) ^{1}H NMR and b) ^{13}C NMR of compd. **7c** in DMSO-d_6.

a)

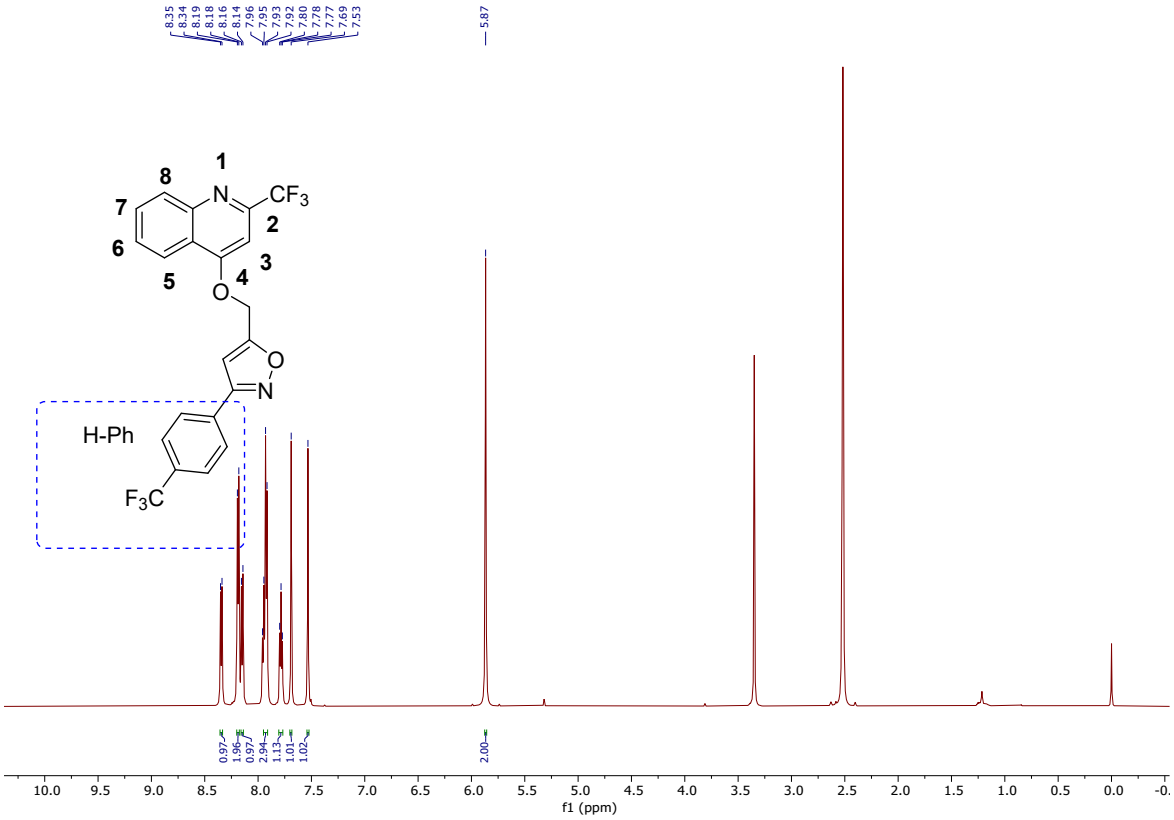

b)

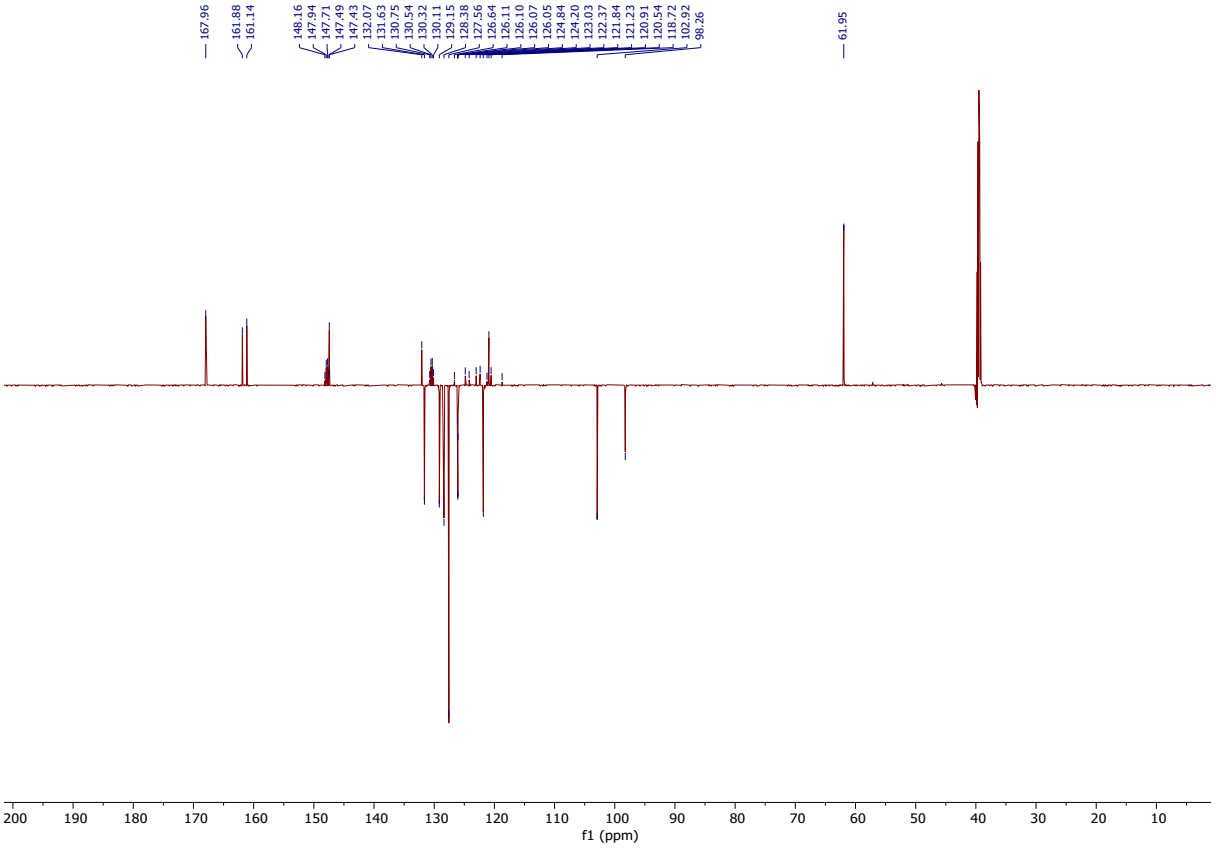

Figure S4: a) ^{1}H NMR and b) ^{13}C NMR of compd. **7d** in DMSO-d_6.

a)

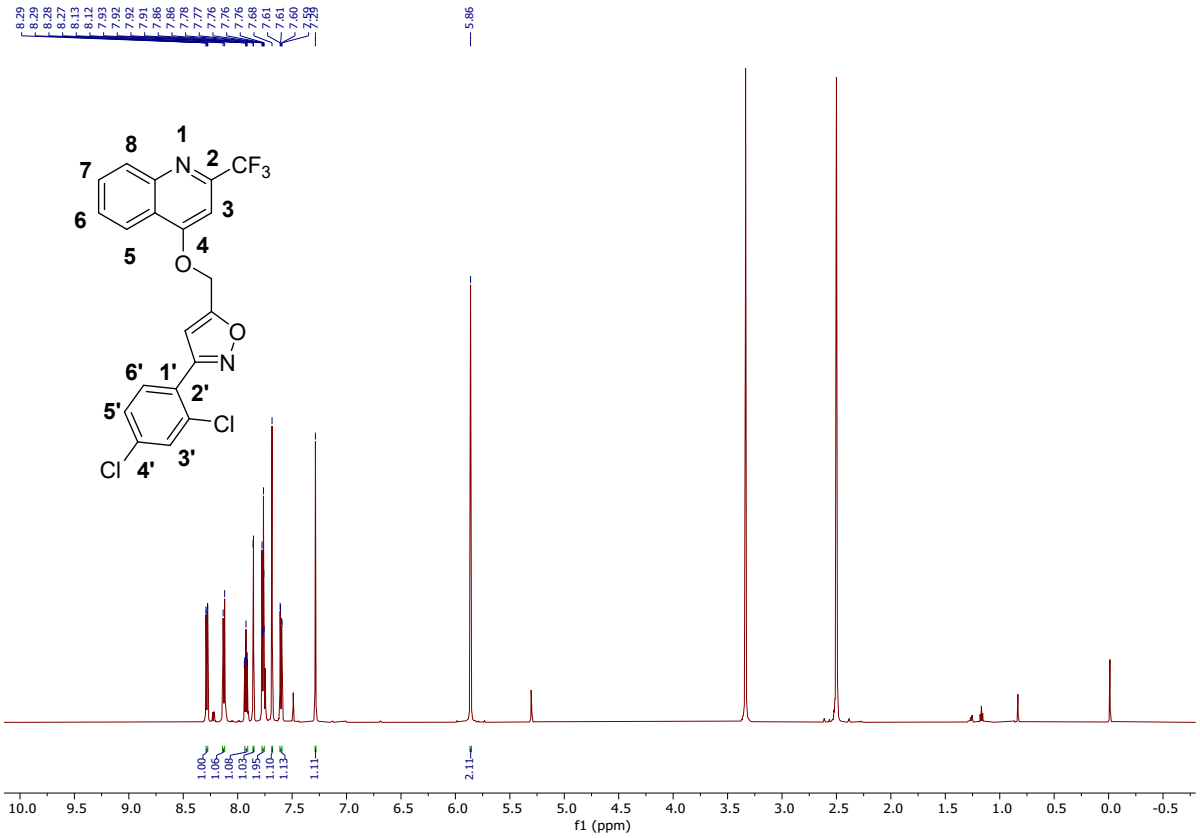

b)

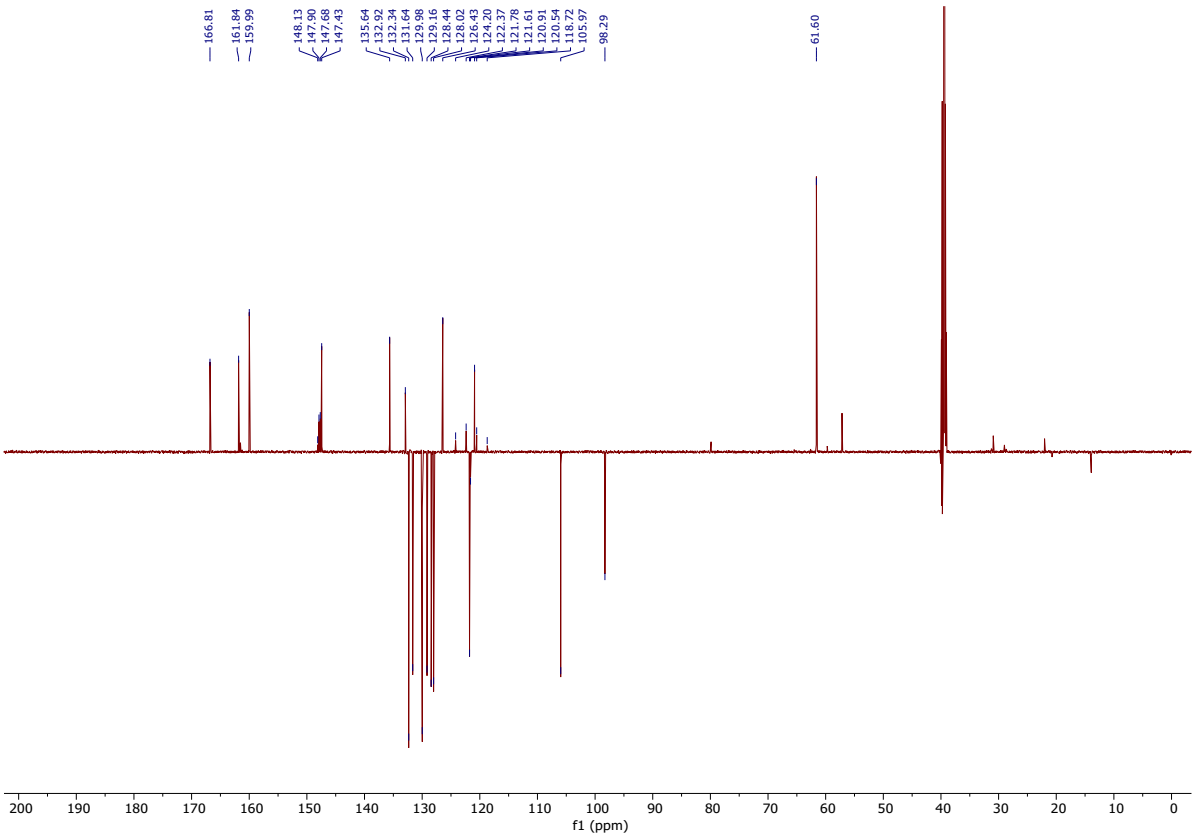

Figure S5: a) ^{1}H NMR and b) ^{13}C NMR of compd. **7e** in DMSO-d_6.

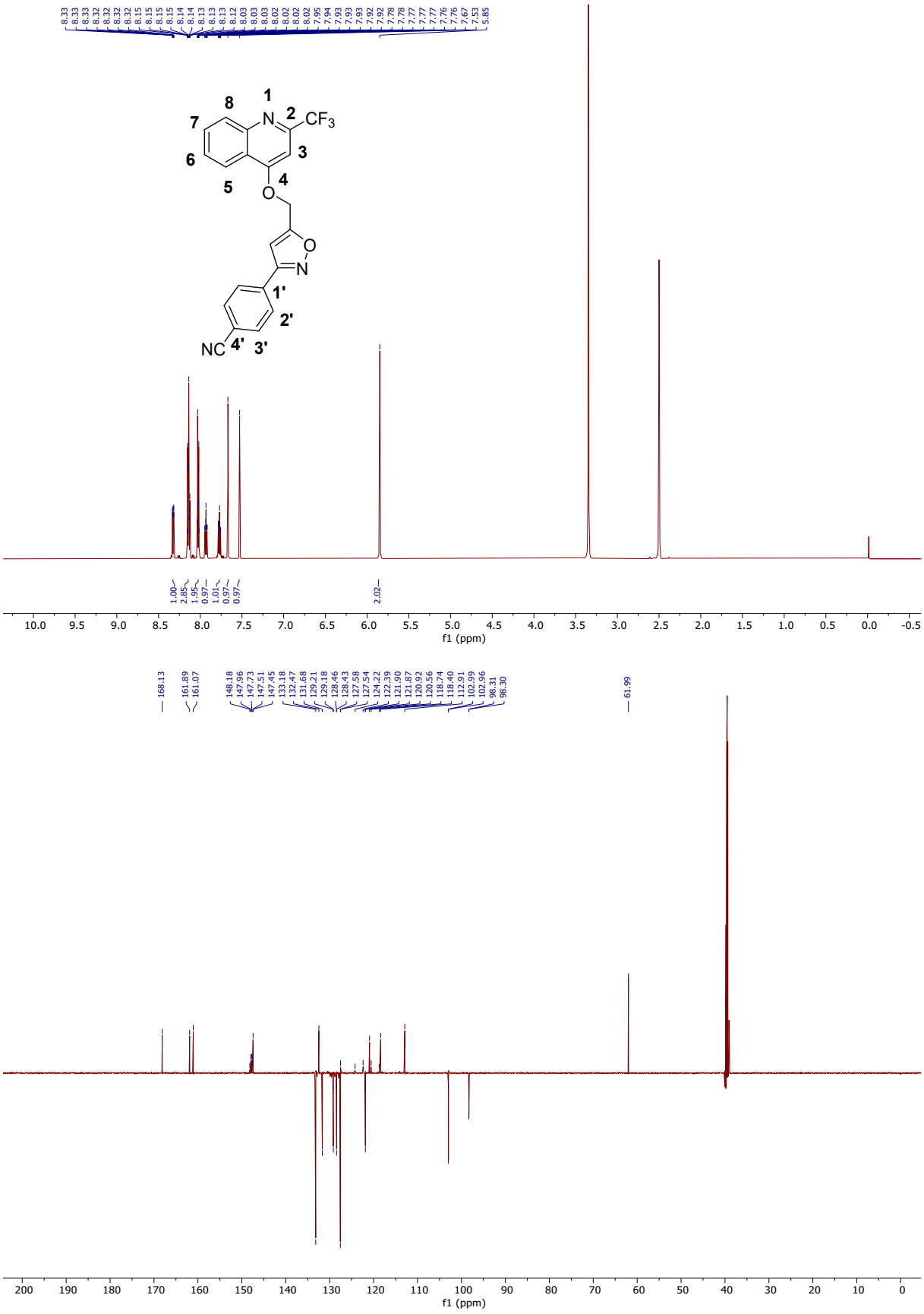

Figure S6: a) ^{1}H NMR and b) ^{13}C NMR of compd. **8a**.

a)

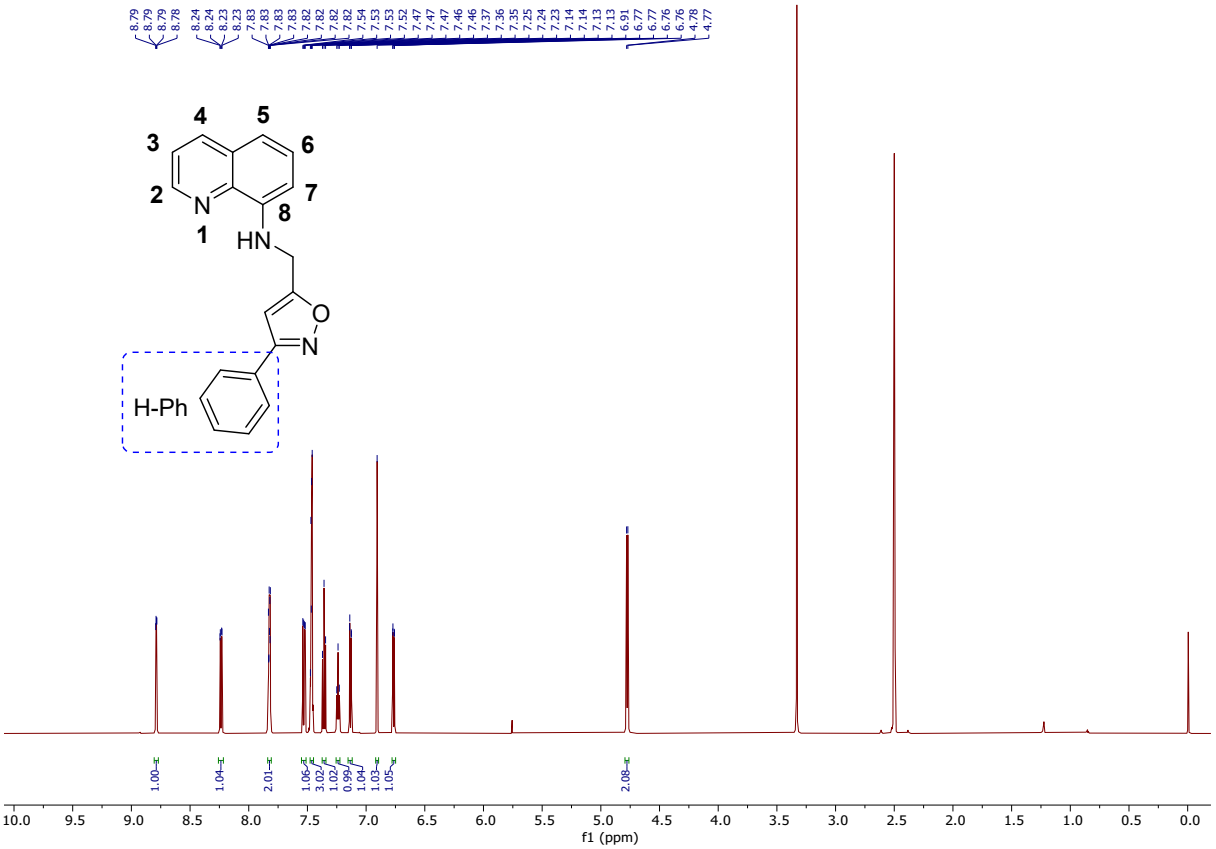

b)

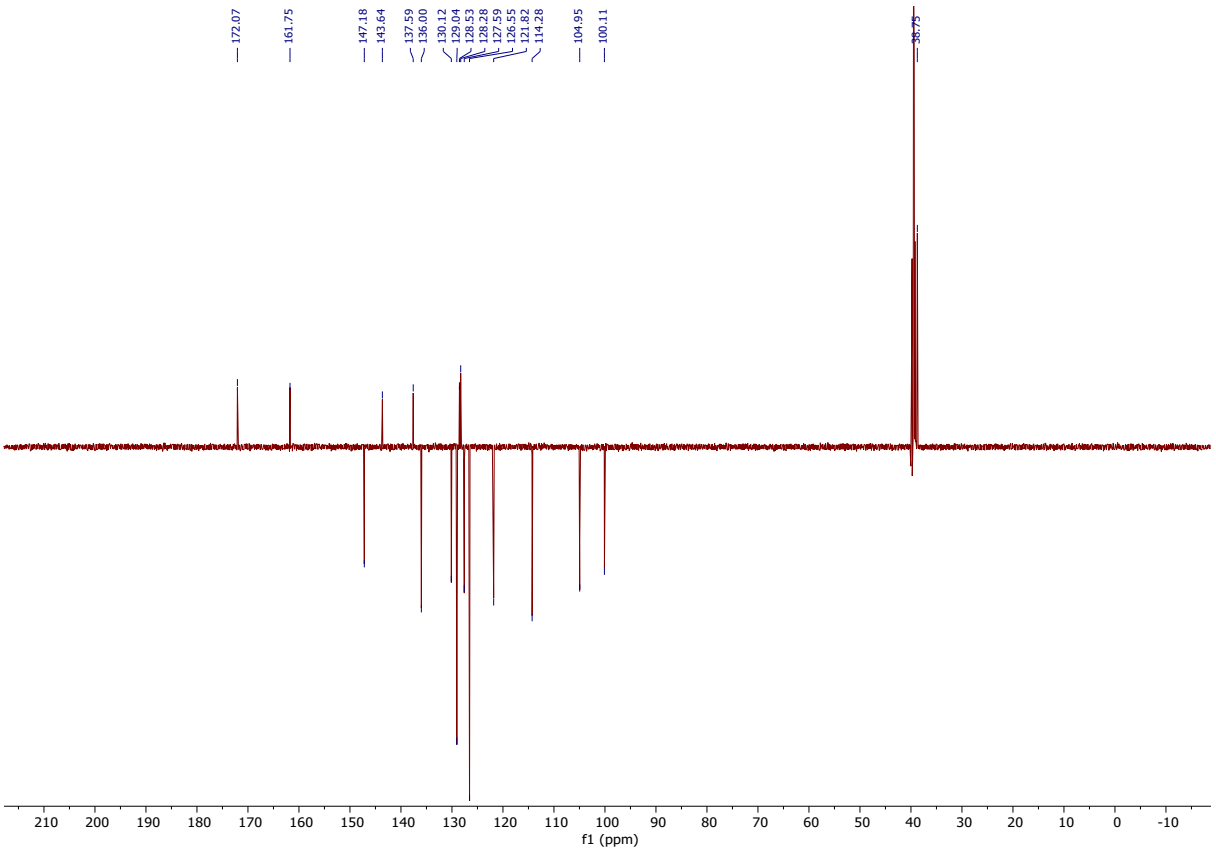

Figure S7: a) ^{1}H NMR and b) ^{13}C NMR of compd. **8b**.

a)

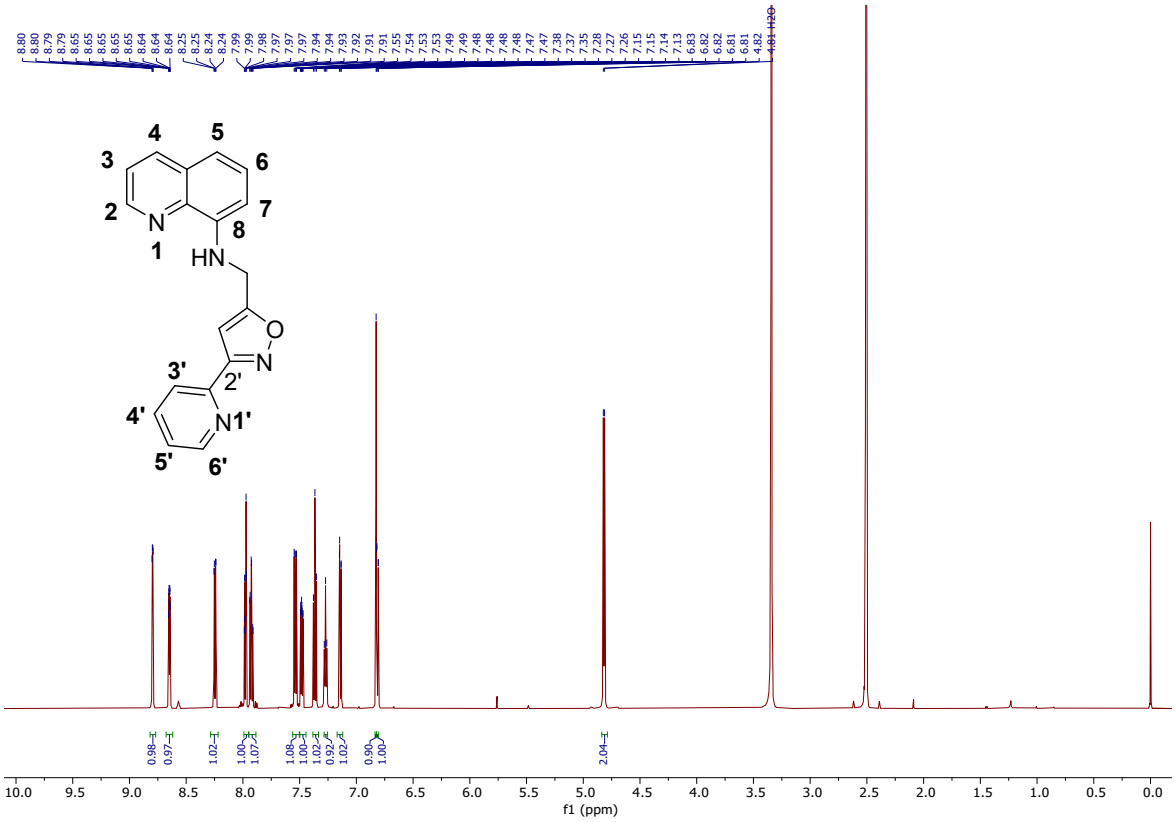

b)

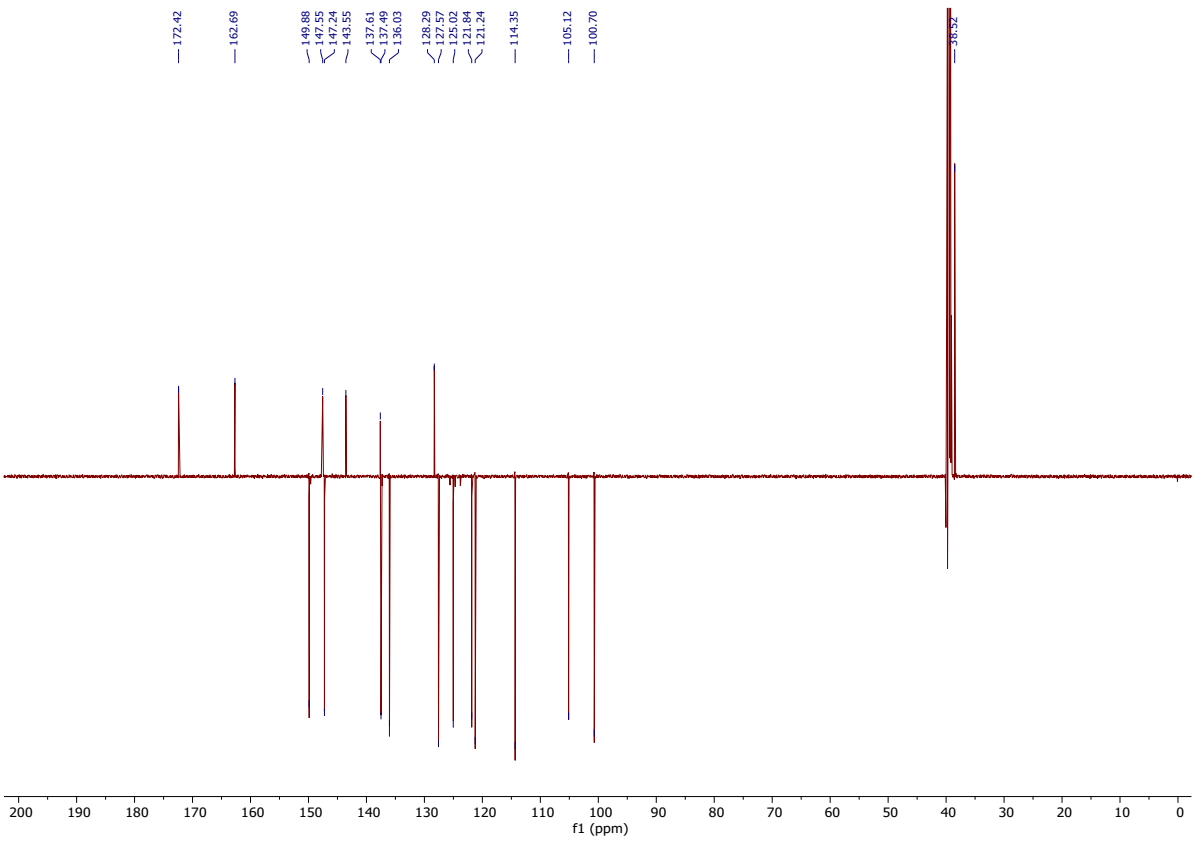

Figure S8: a) ^{1}H NMR and b) ^{13}C NMR of compd. **8c**.

a)

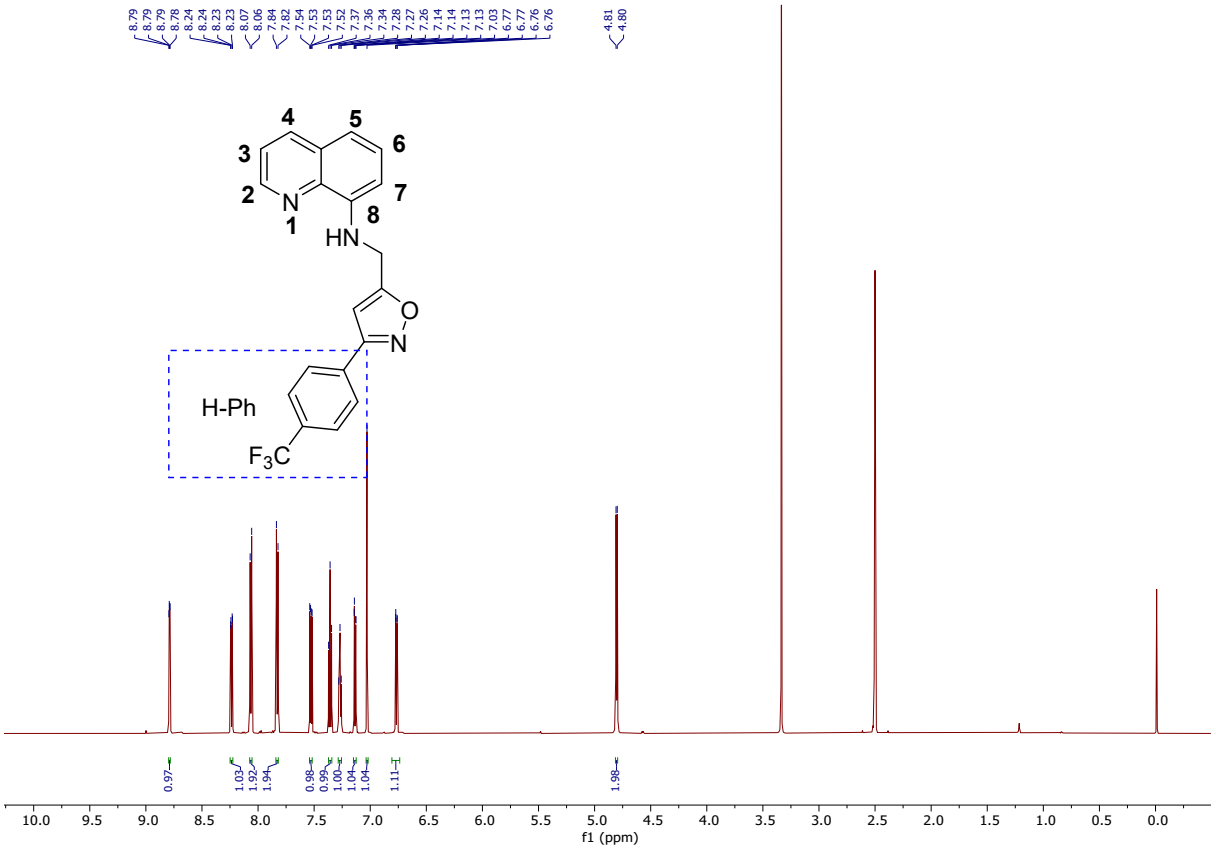

b)

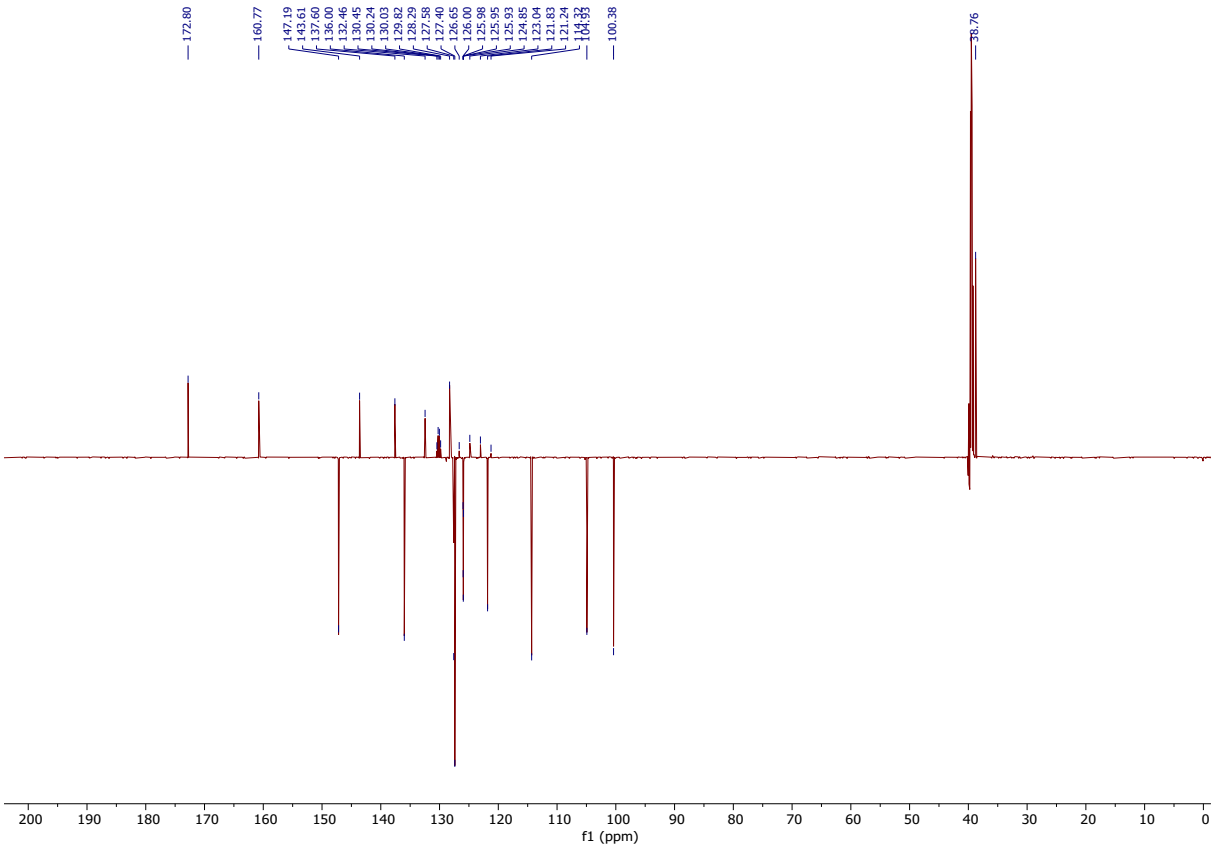

Figure S9: a) ^{1}H NMR and b) ^{13}C NMR of compd. **8d**.

a)

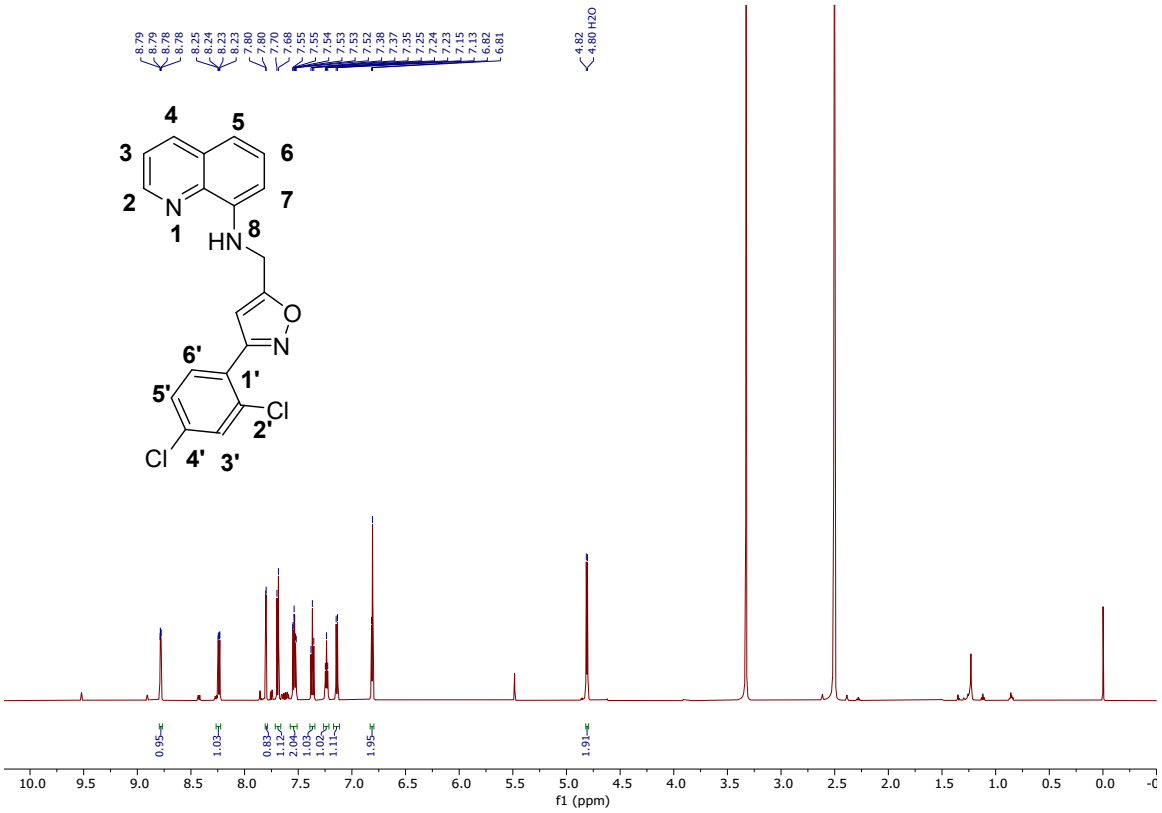

b)

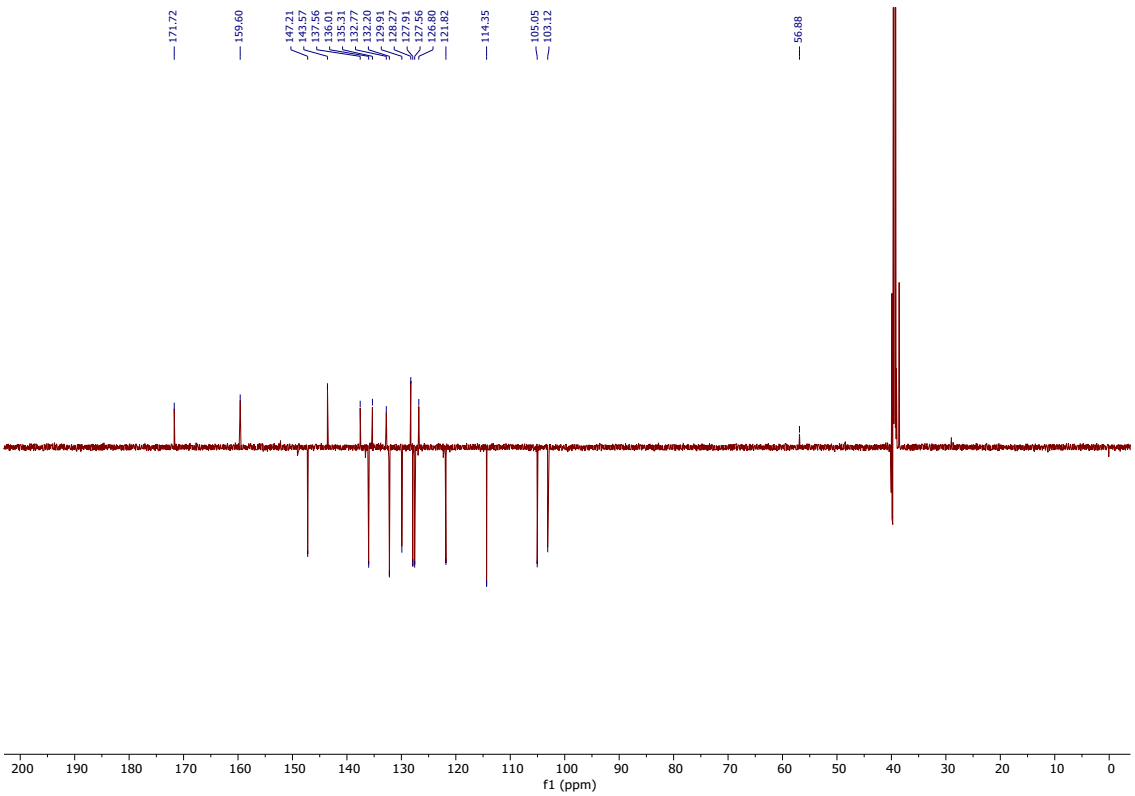

Figure S10: a) ^{1}H NMR and b) ^{13}C NMR of compd. **8e**.

a)

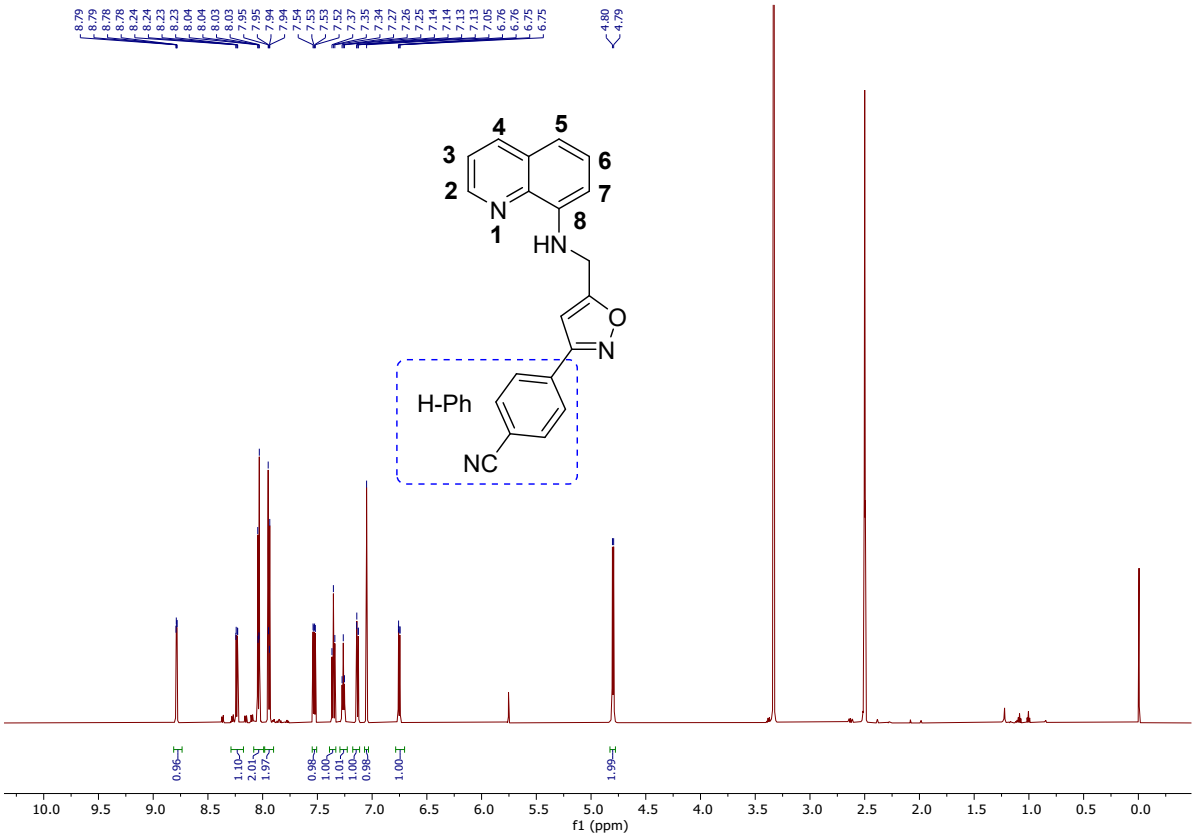

b)

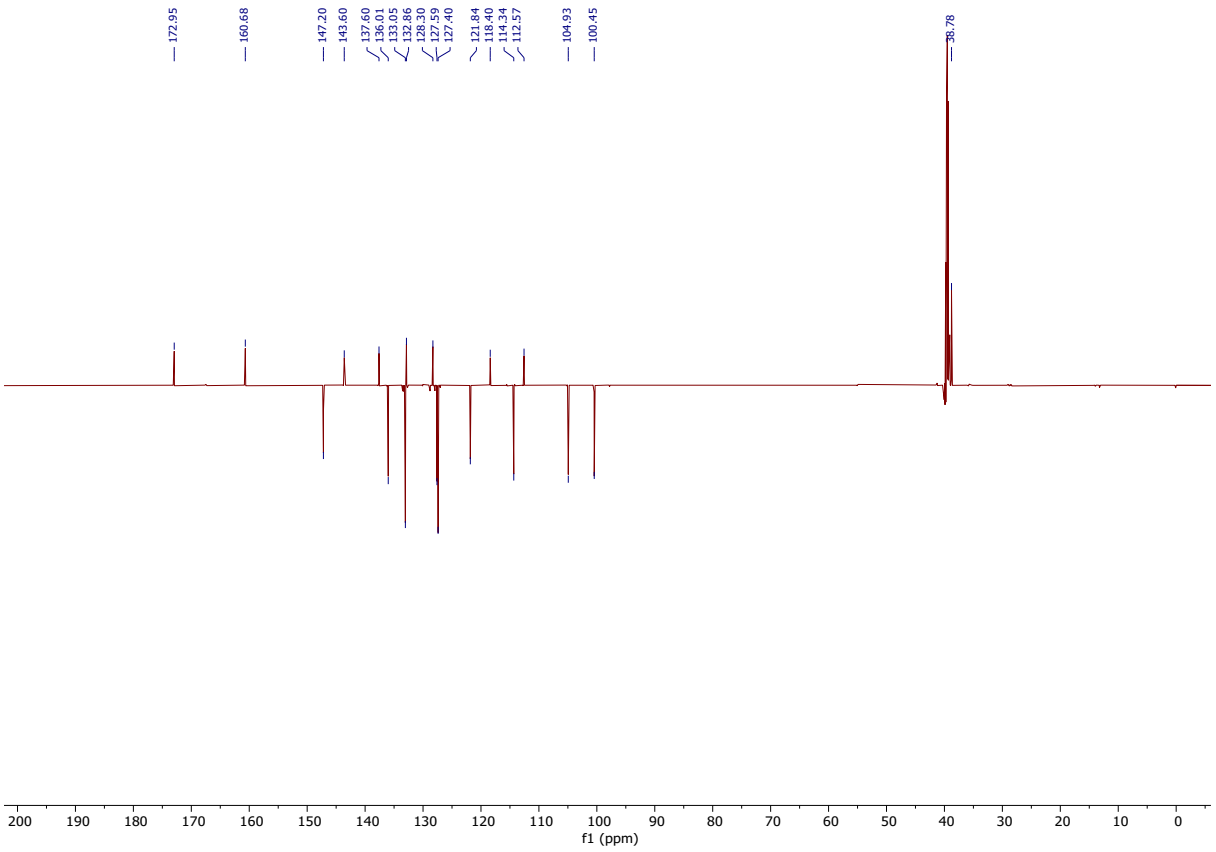

Figure S11: a) ^{1}H NMR and b) ^{13}C NMR of compd. **8f**.

a)

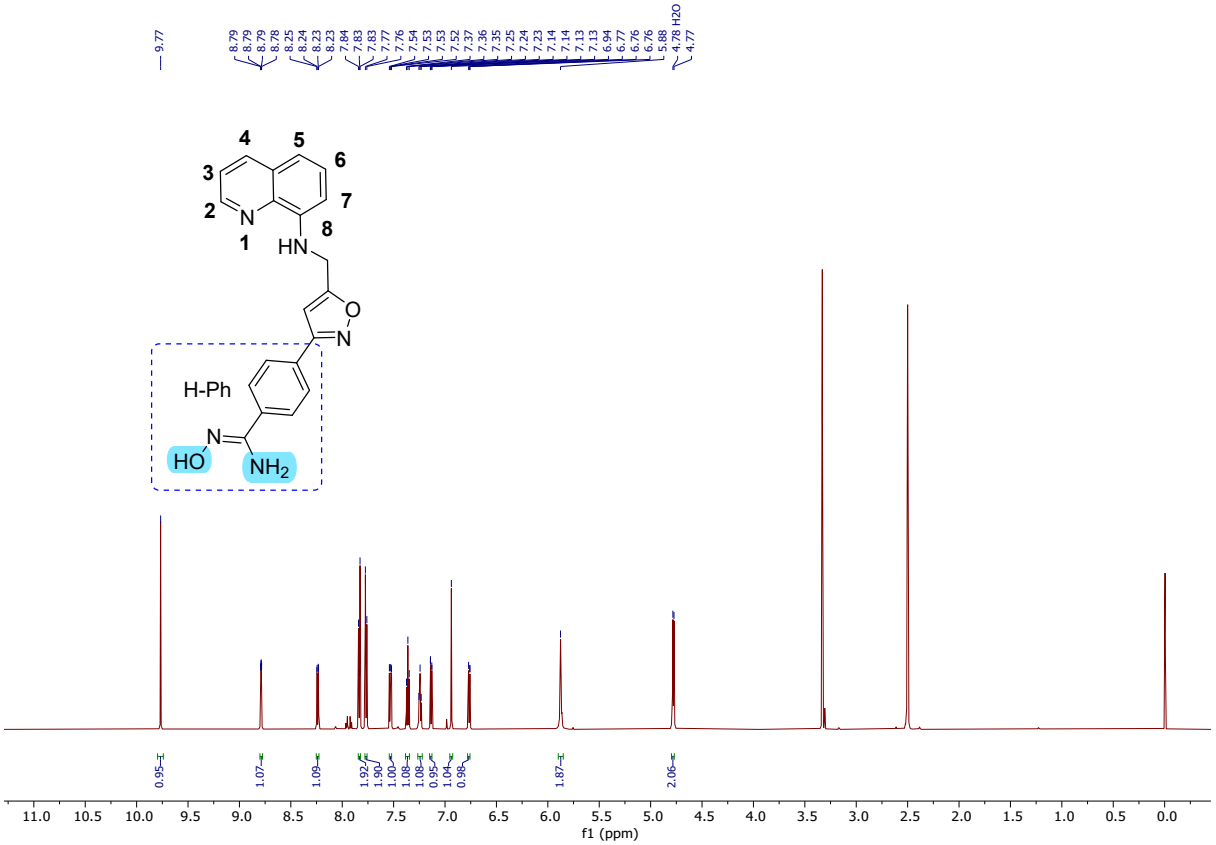

b)

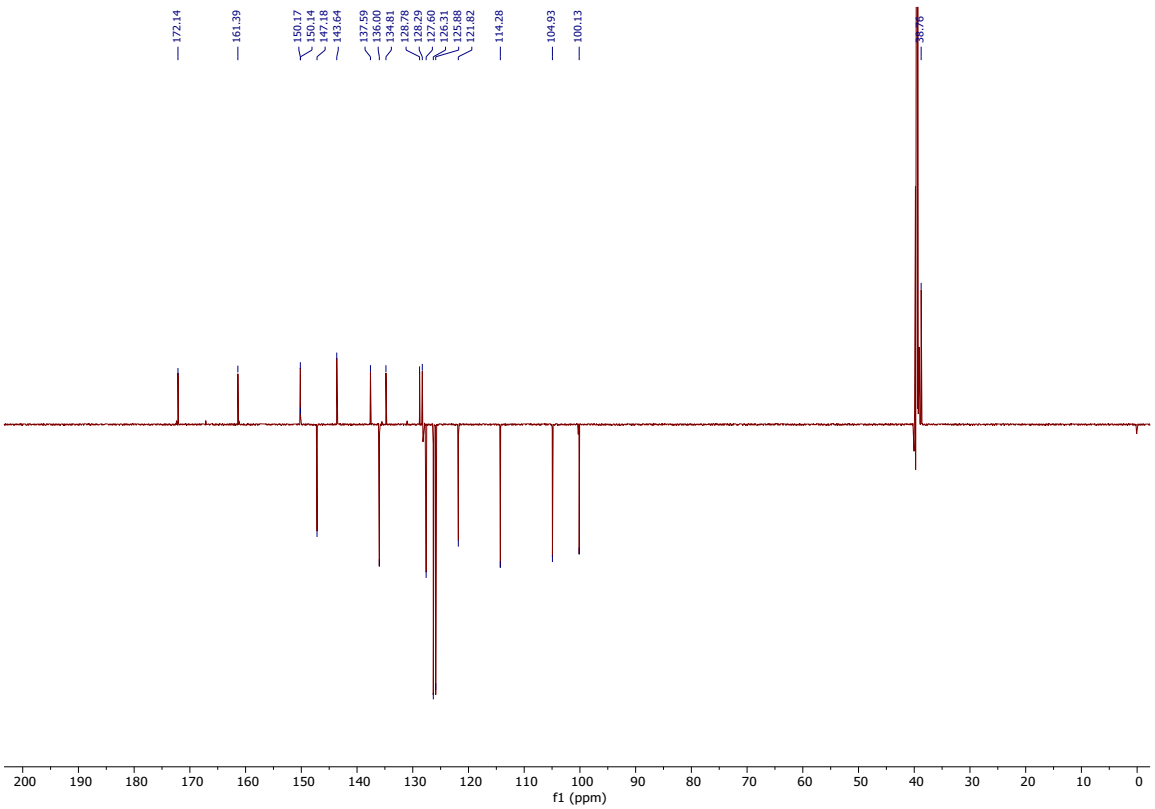

Figure S12: a) ^{1}H NMR and b) ^{13}C NMR of compd. **9a**.

a)

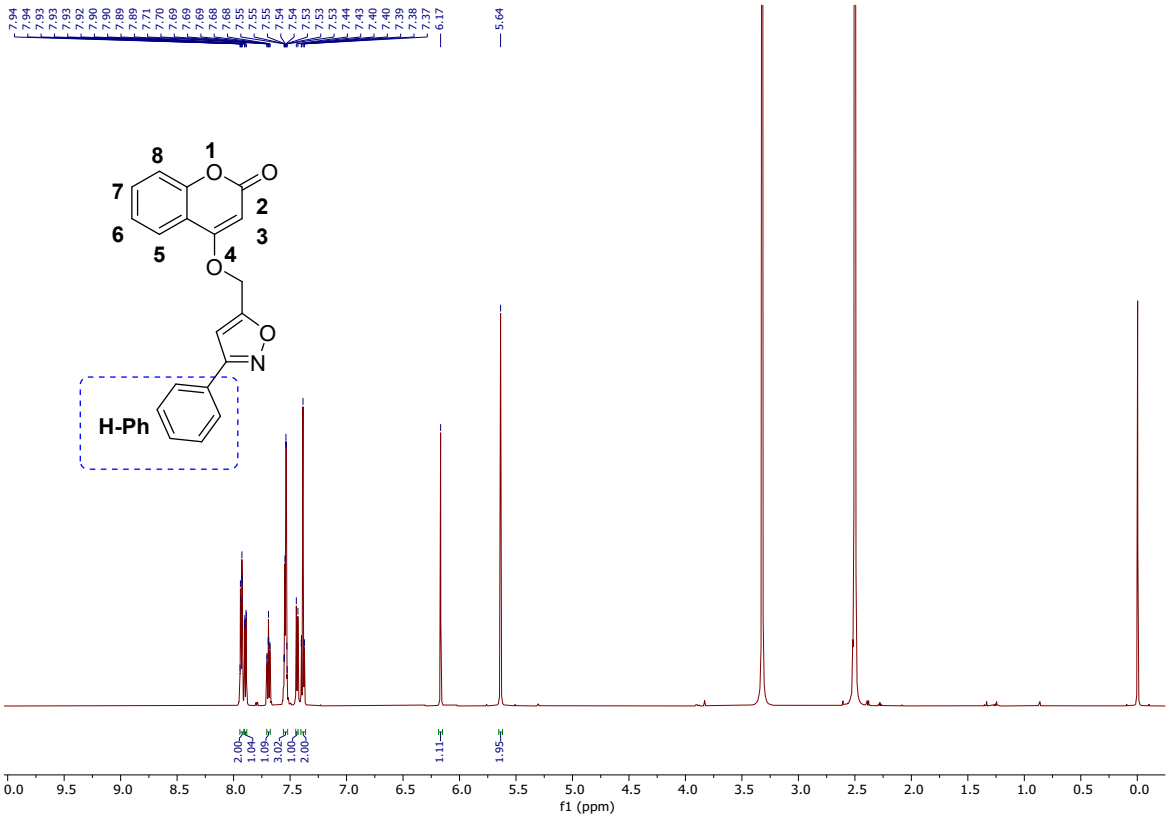

b)

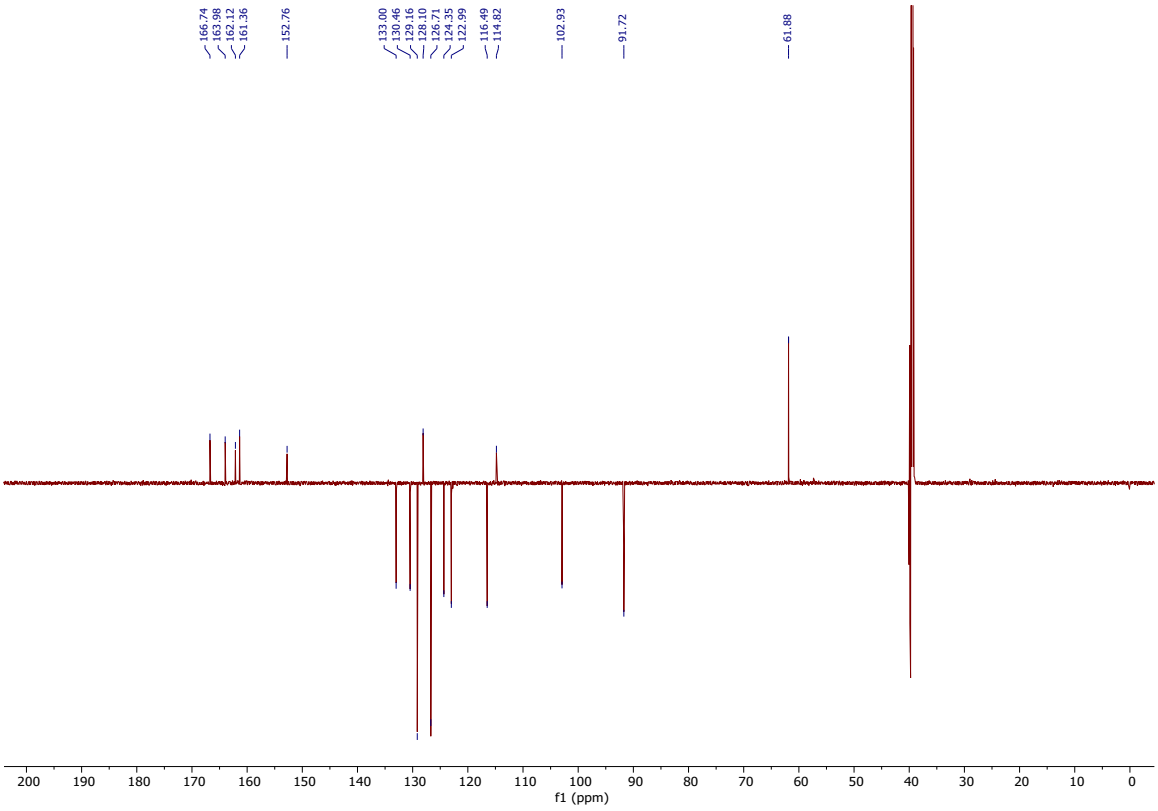

Figure S13: a) ^{1}H NMR and b) ^{13}C NMR of compd. **9b**.

a)

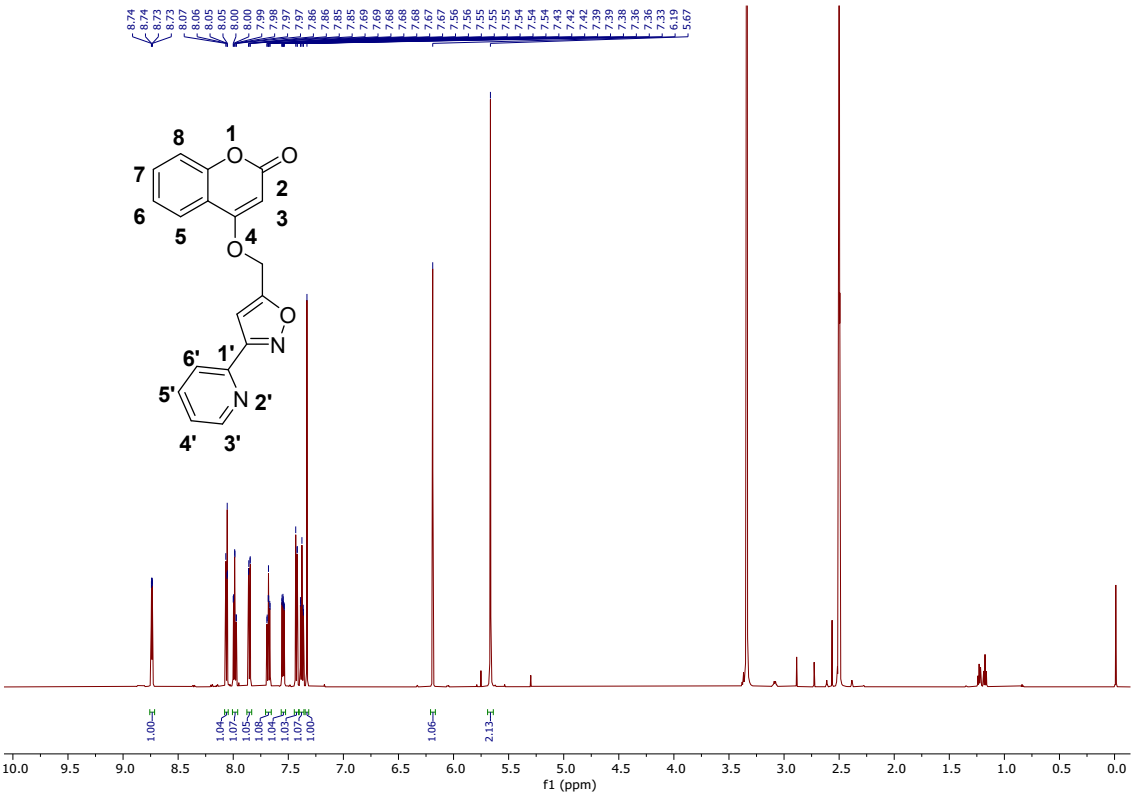

b)

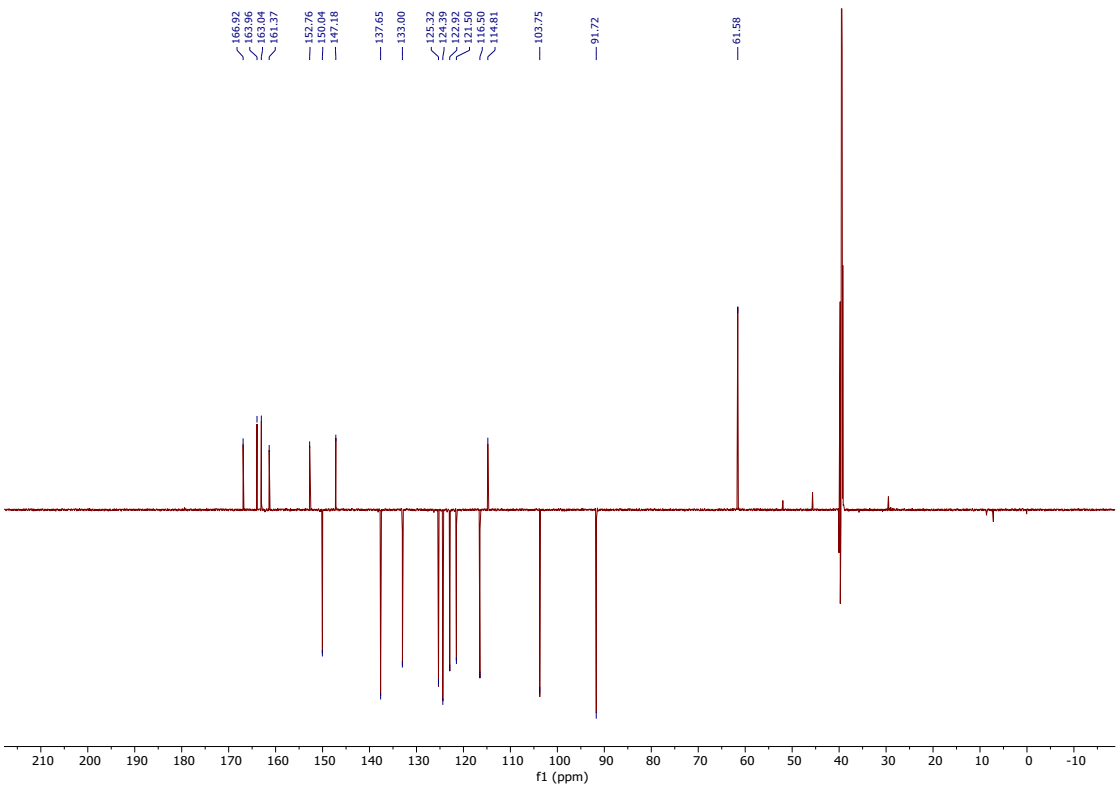

Figure S14: a) ^{1}H NMR and b) ^{13}C NMR of compd. **9c**.

a)

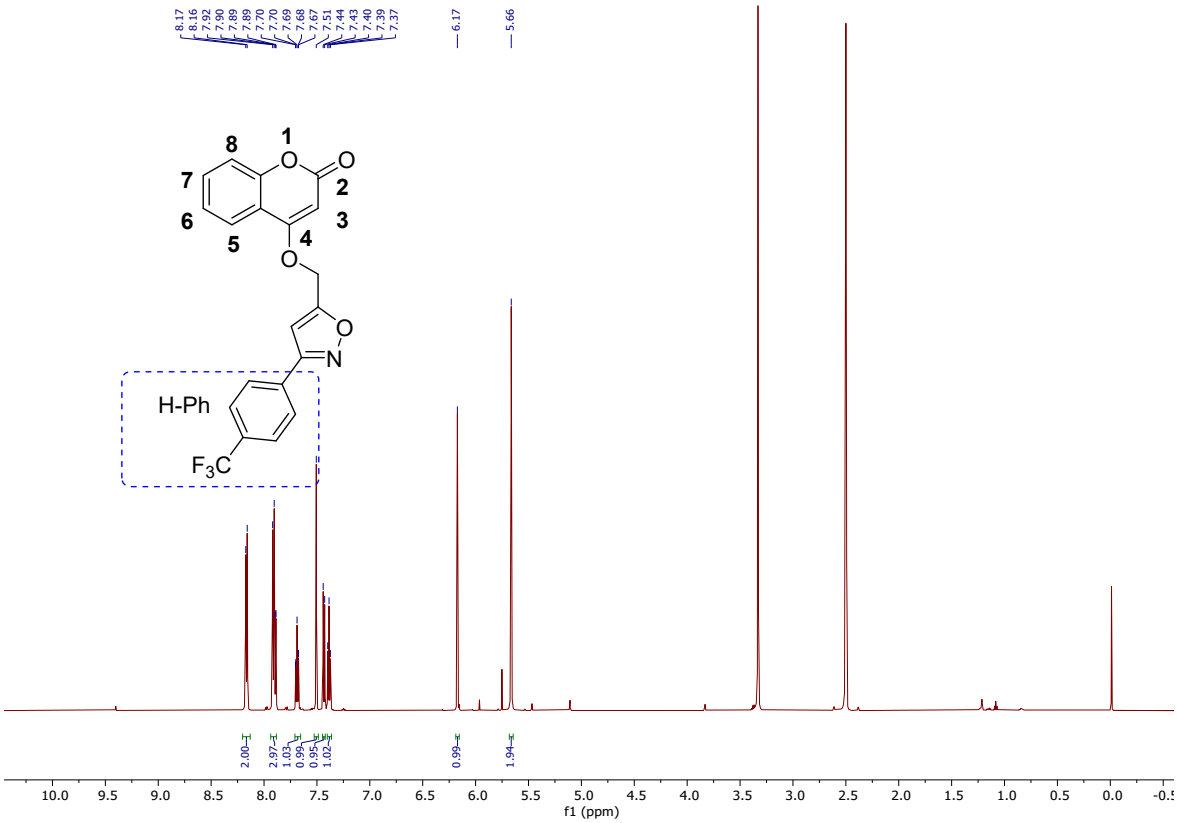

b)

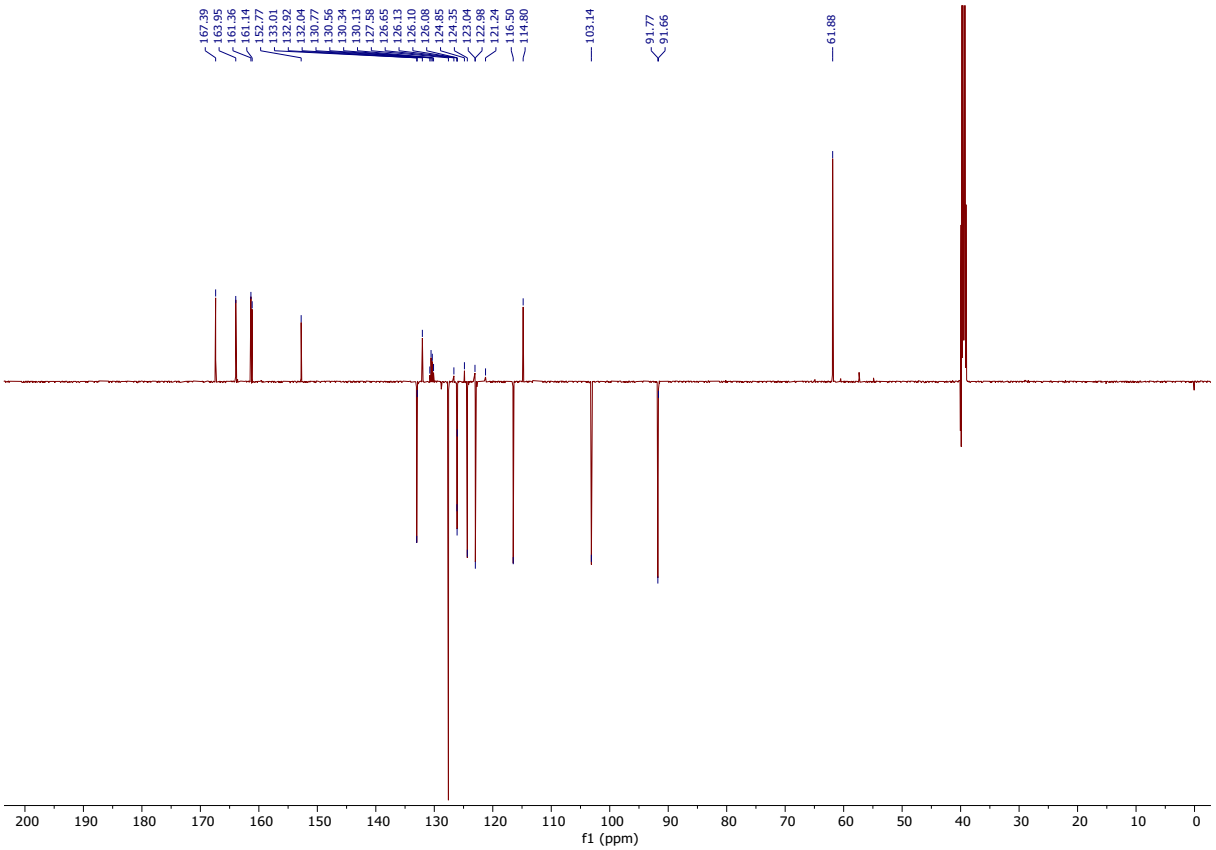

Figure S15: a) ^{1}H NMR and b) ^{13}C NMR of compd. **9d**.

a)

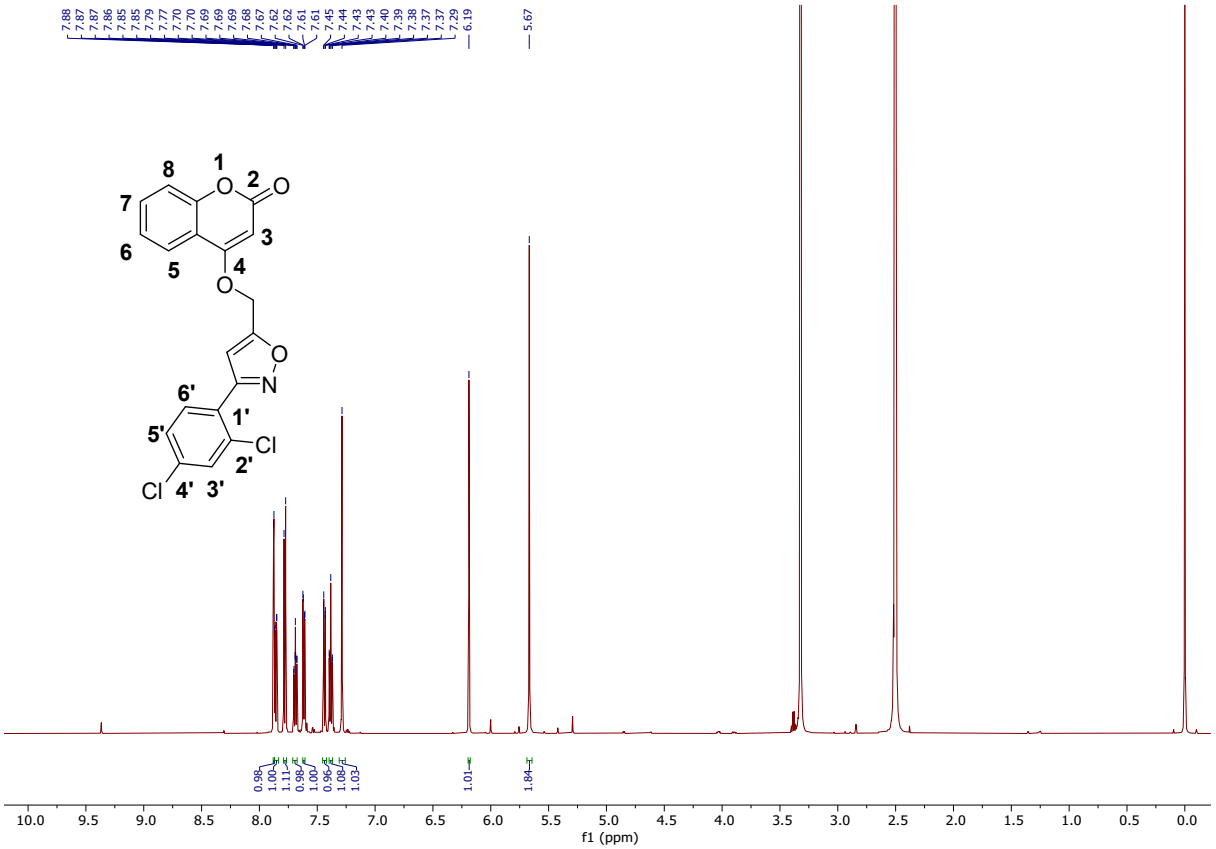

b)

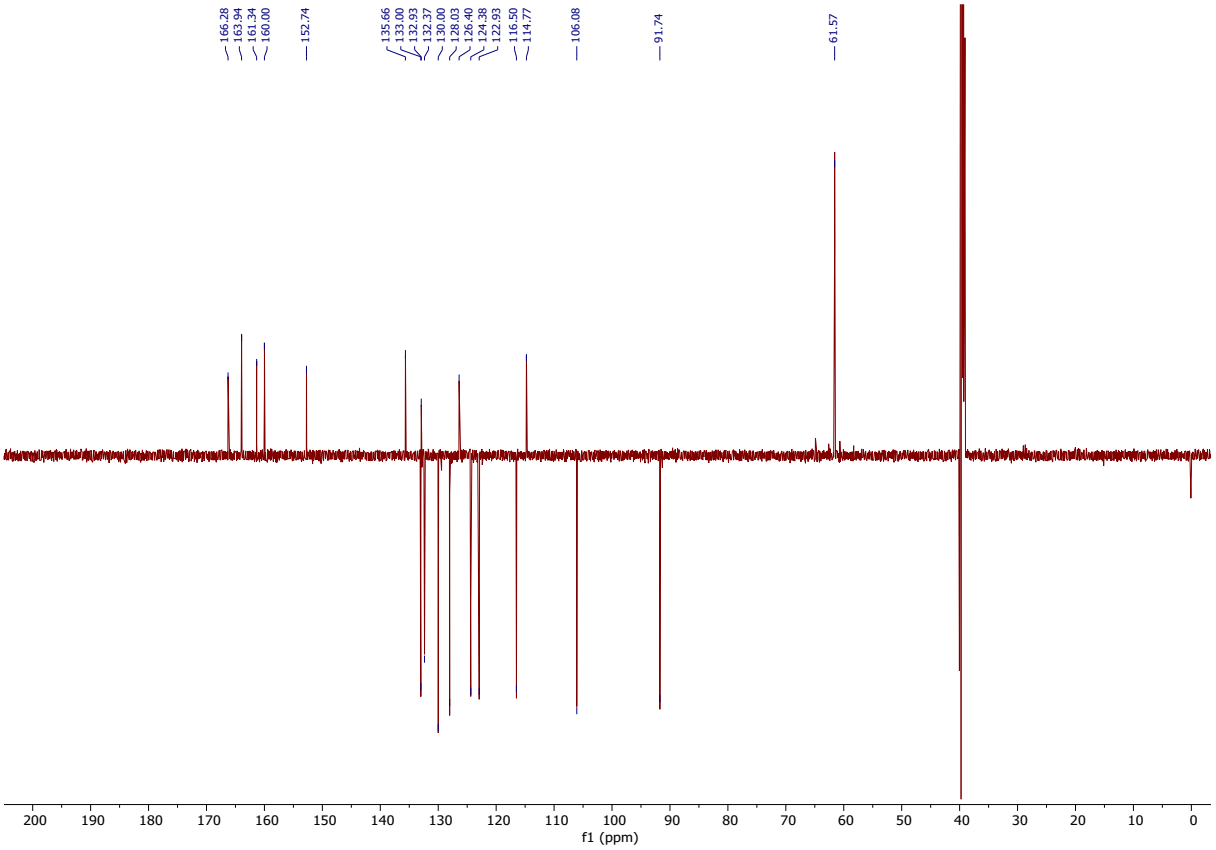

Figure S16: a) ^{1}H NMR and b) ^{13}C NMR of compd. **9e**.

a)

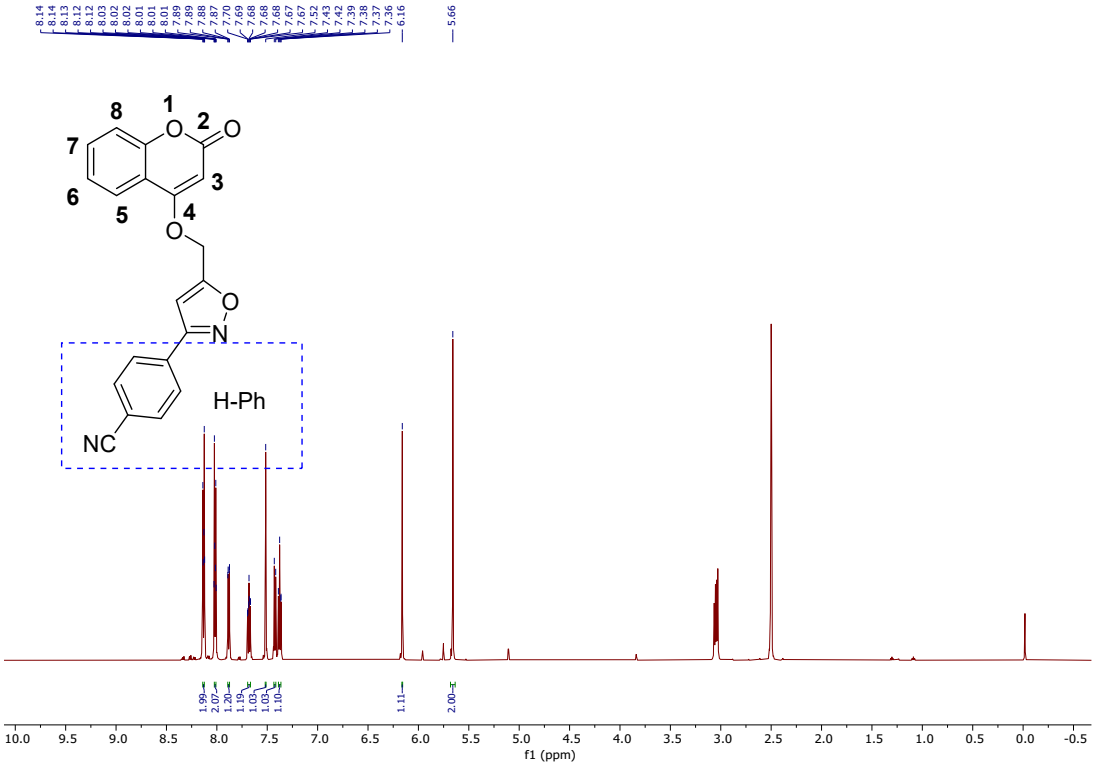

b)

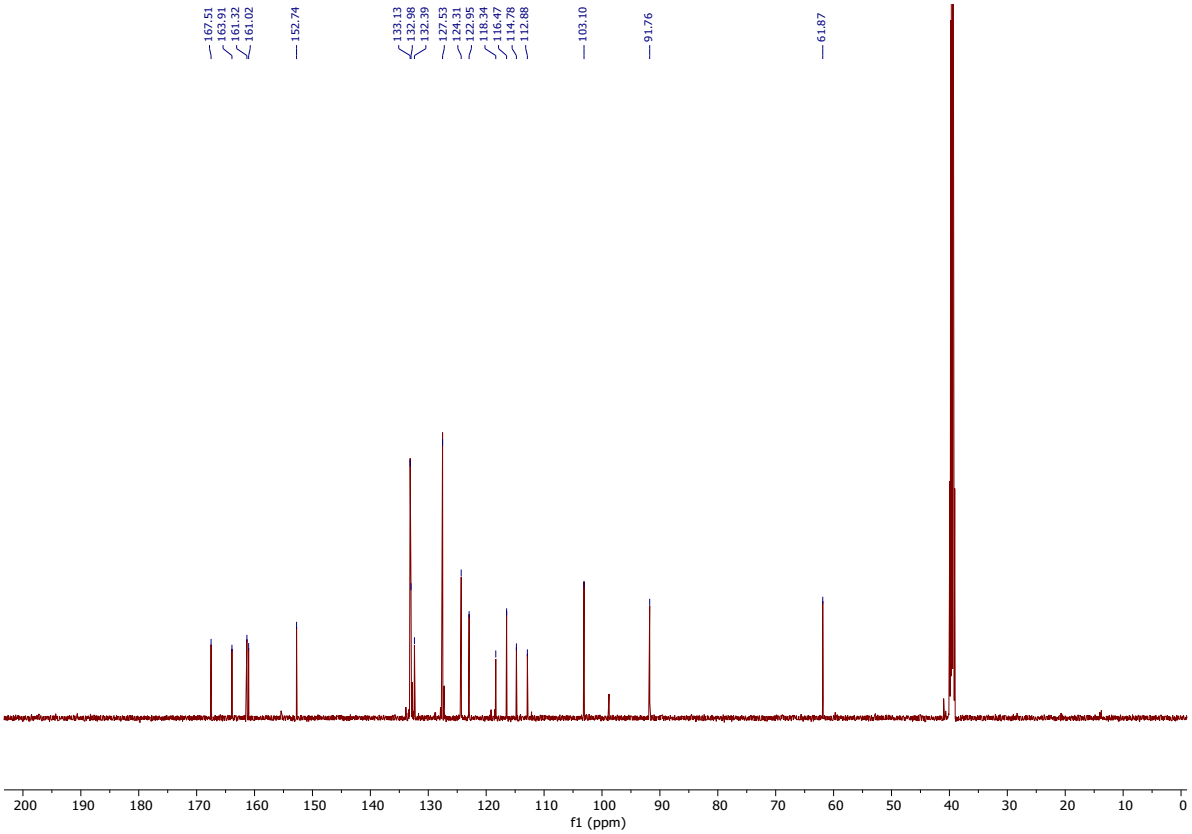

1.2. ^{1}H and ^{13}C NMR spectra of Re(I) ($7b_{Re}$, $9b_{Re}$) and Ru(II) ($7b_{Ru}$, $9b_{Ru}$) complexes

Figure S17: a) ^{1}H NMR and b) ^{13}C NMR of compd **$7b_{Re}$**.

a)

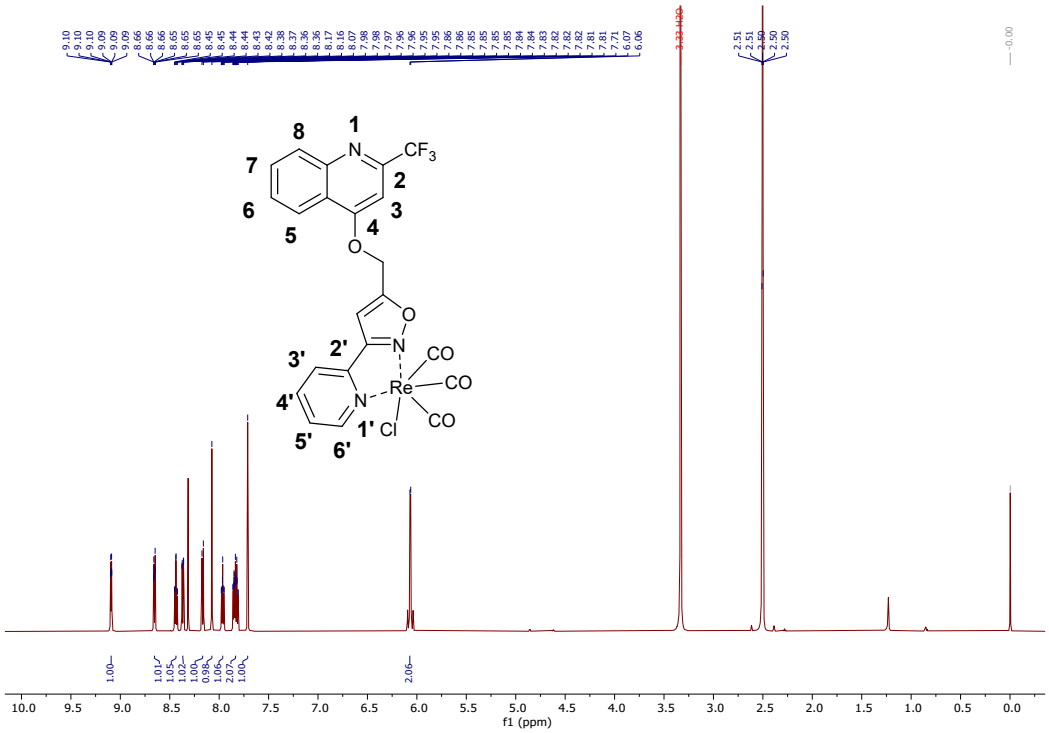

b)

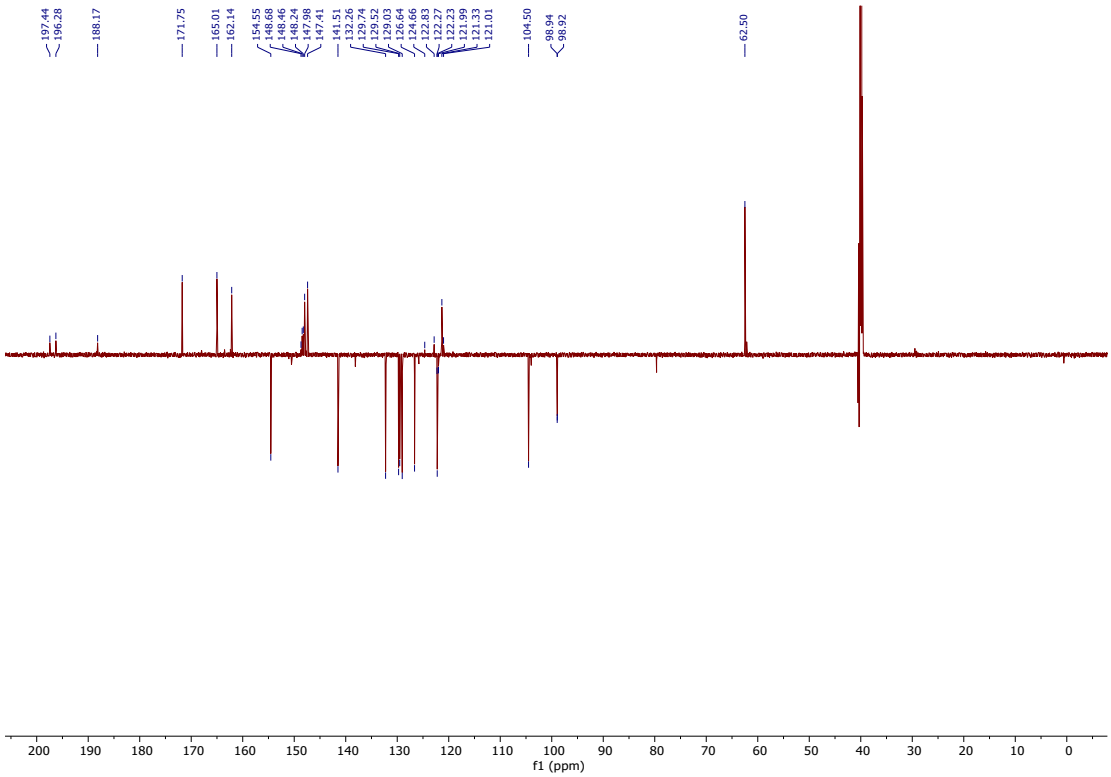

Figure S18: a) ^{1}H NMR and b) ^{13}C NMR of compd **9b$_{Re}$**.

a)

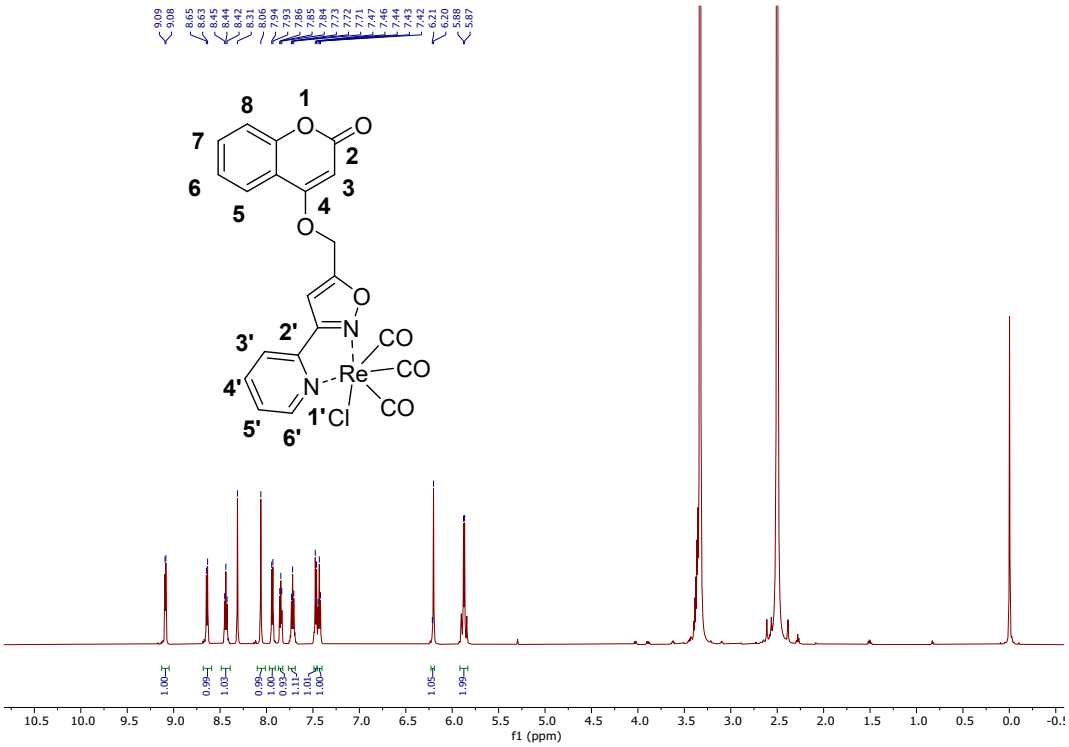

b)

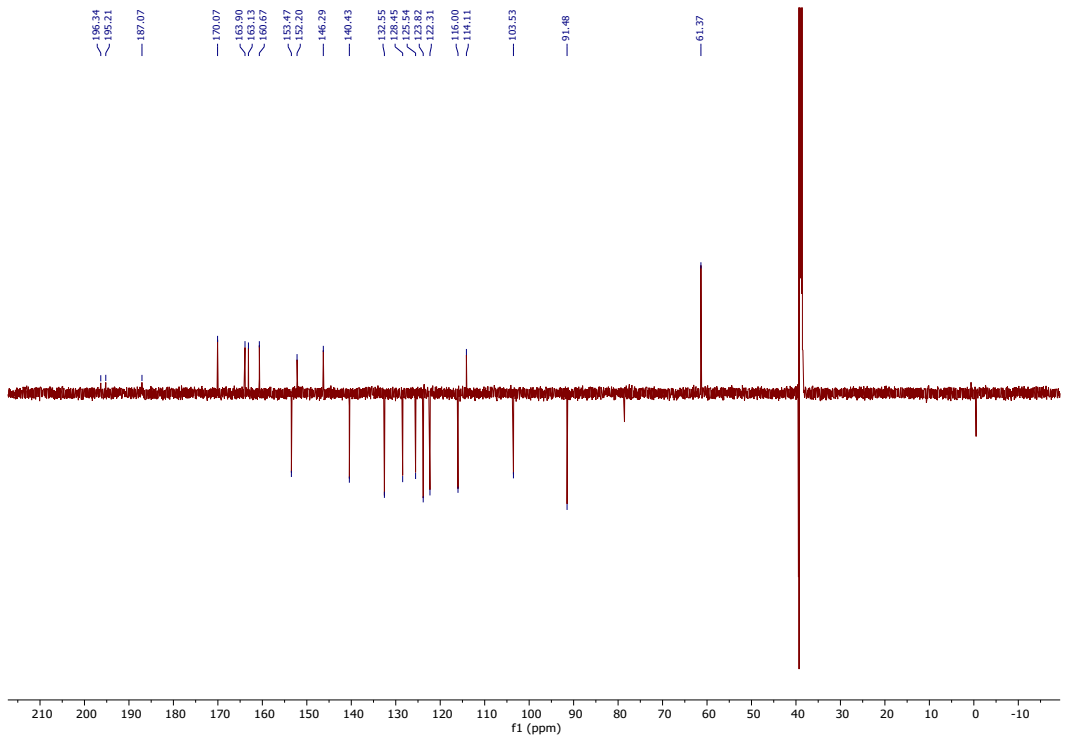

Figure S19: a) ^{1}H NMR and b) ^{13}C NMR of compd. **7b$_{Ru}$**.

a)

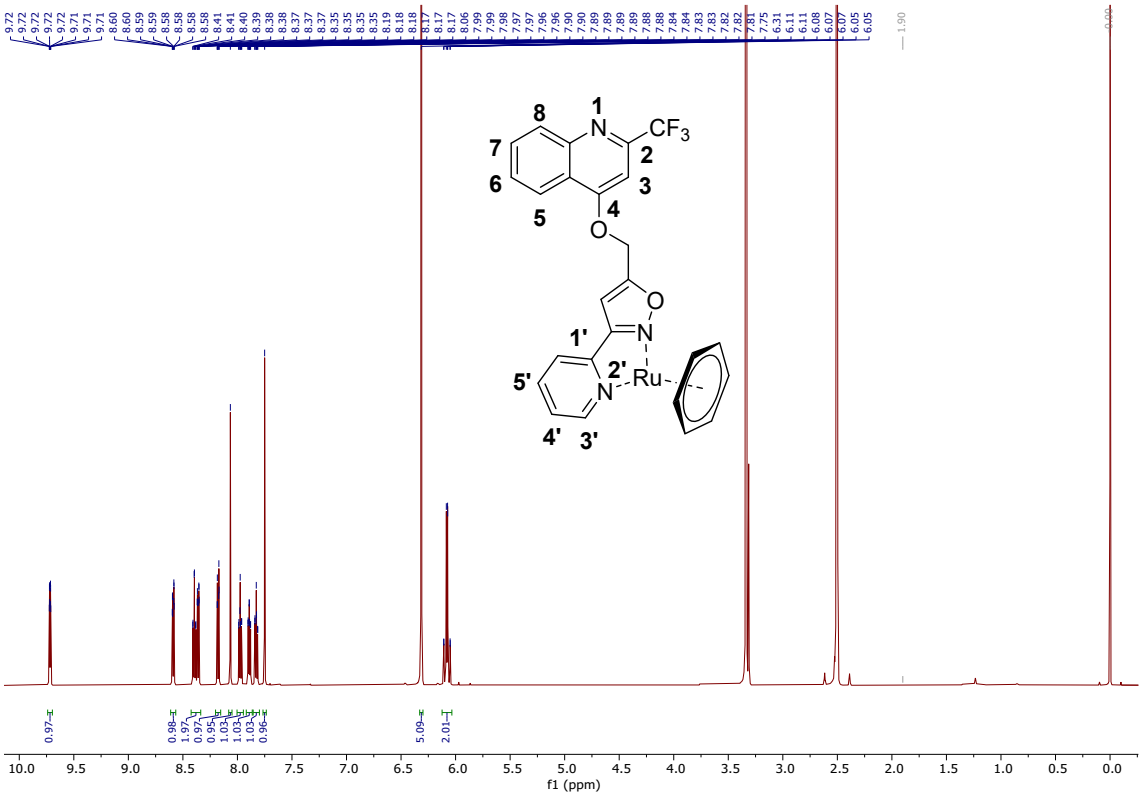

b)

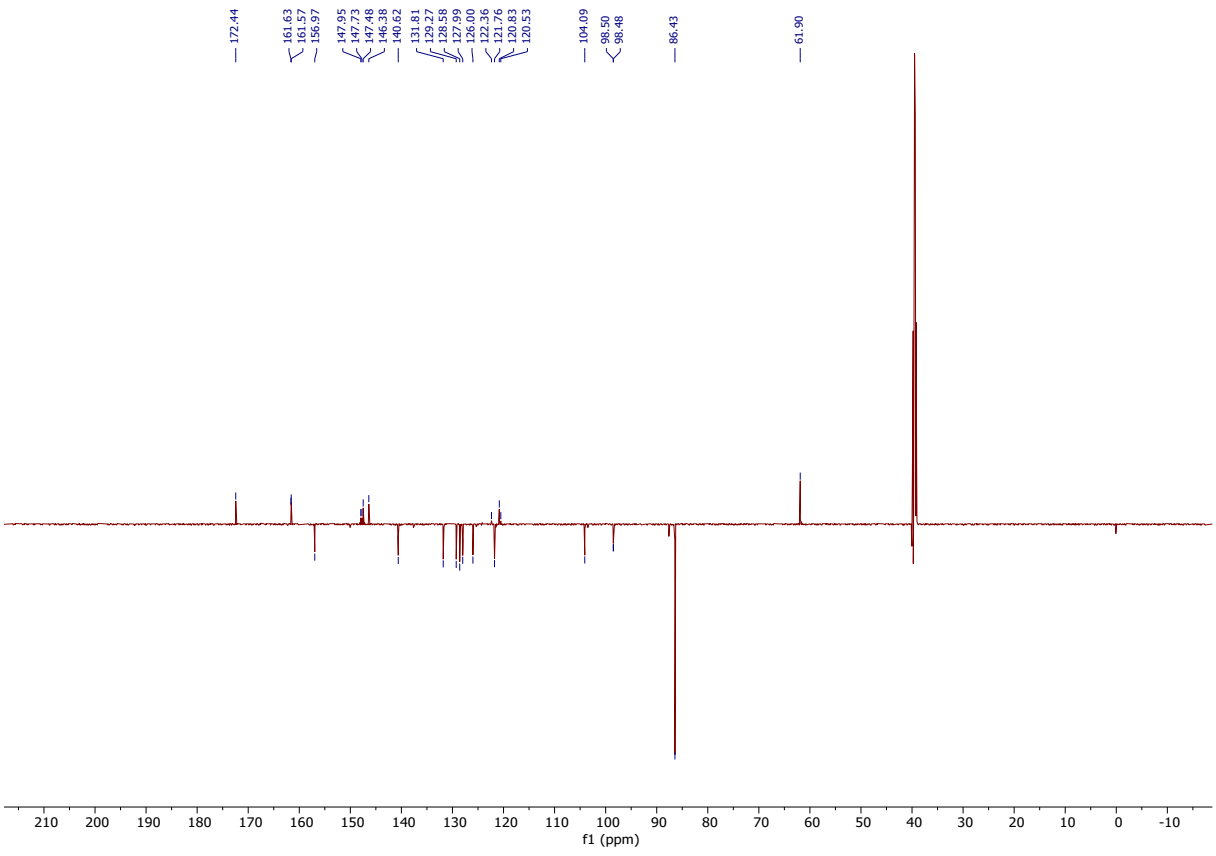

Figure S20: a) ^{1}H NMR and b) ^{13}C NMR of compd. **$9b_{Ru}$**.

a)

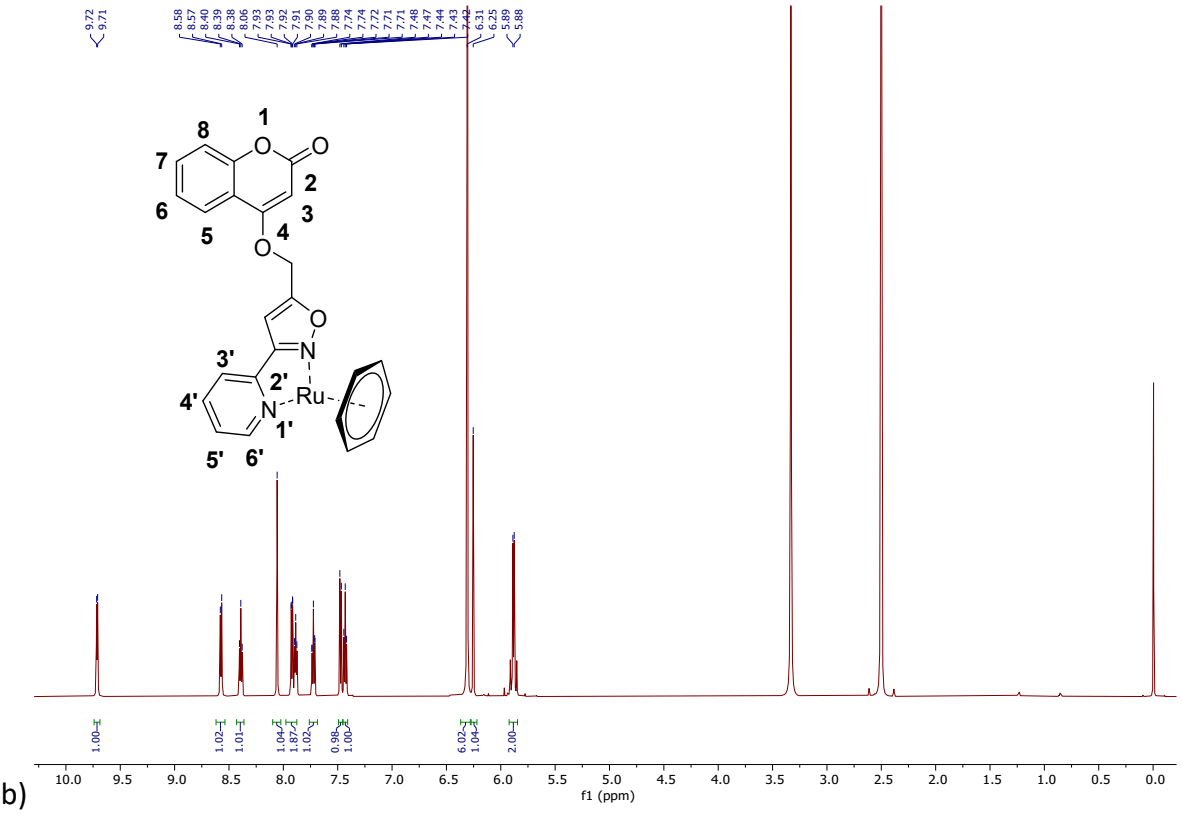

b)

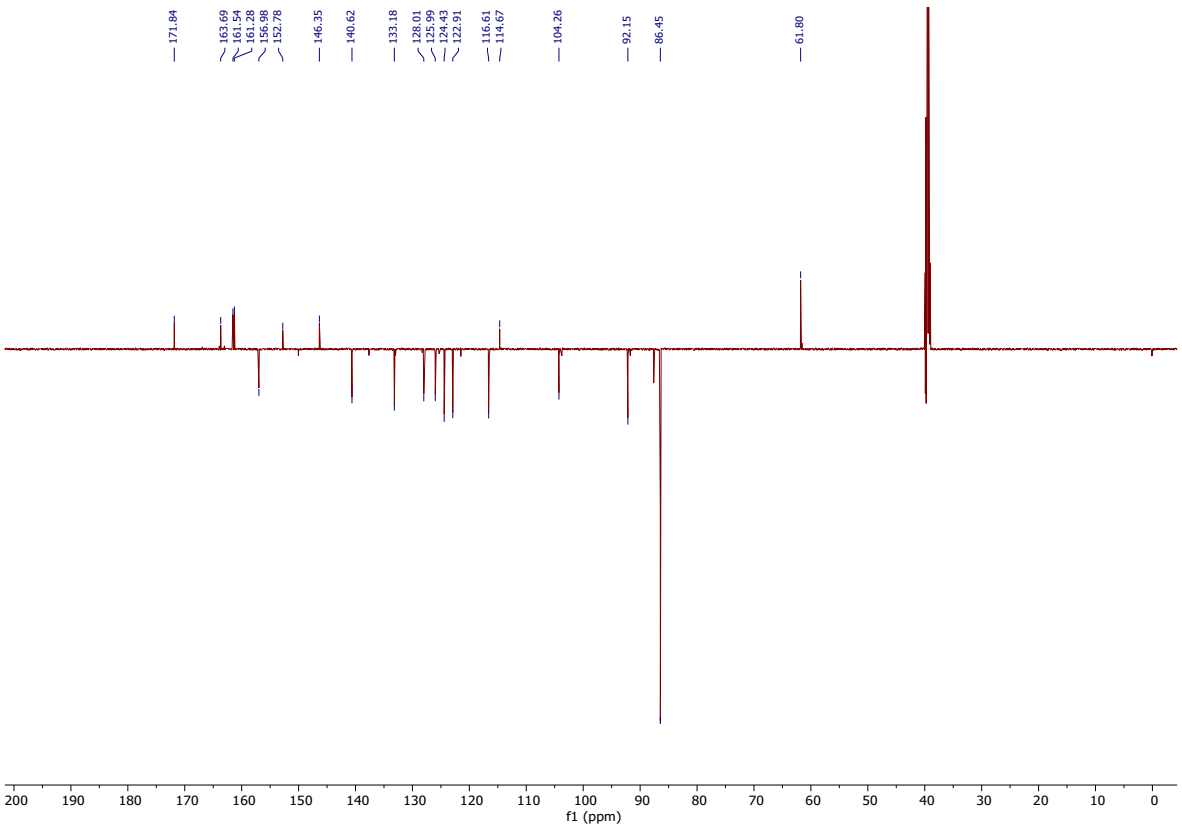

2. FTIR spectra of ligands (7b, 9b) and complexes ($7b_{Re}$, $7b_{Ru}$, $9b_{Re}$, $9b_{Ru}$)

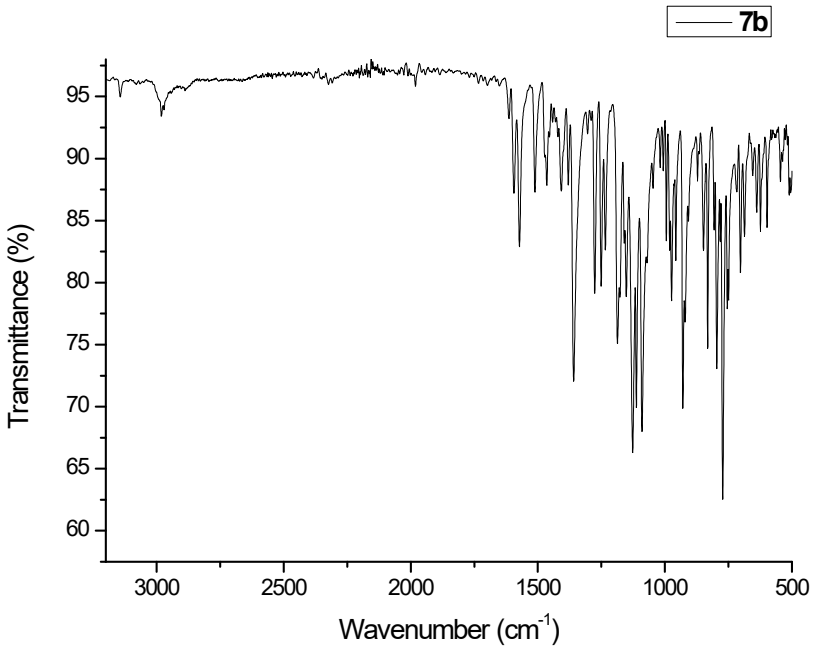

Figure S21. FTIR spectrum of **7b**.

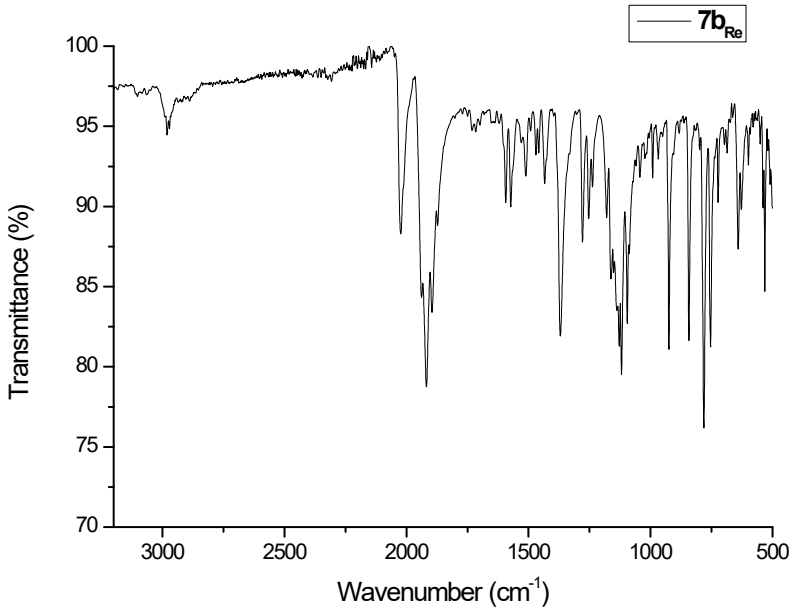

Figure S22. FTIR spectrum of $\mathbf{7b_{Re}}$.

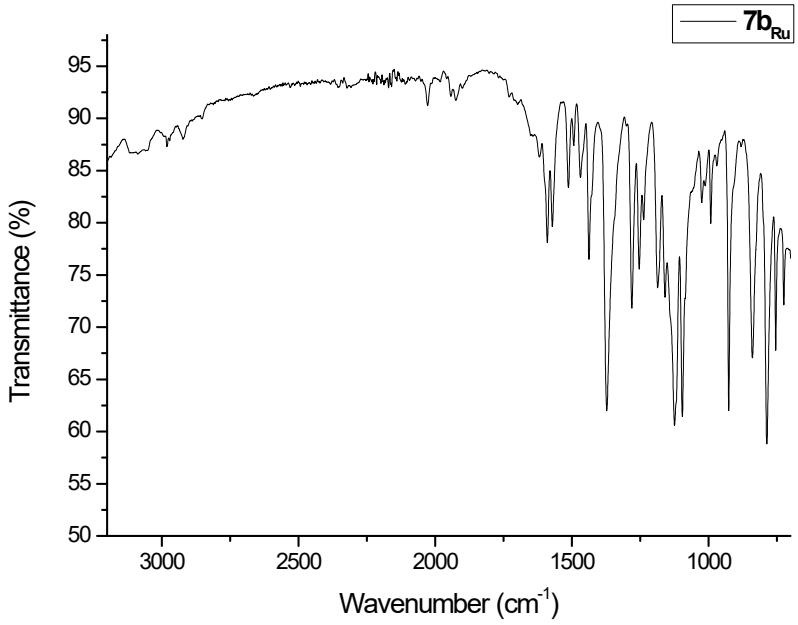

Figure S23. FTIR spectrum of **7b$_{Ru}$.**

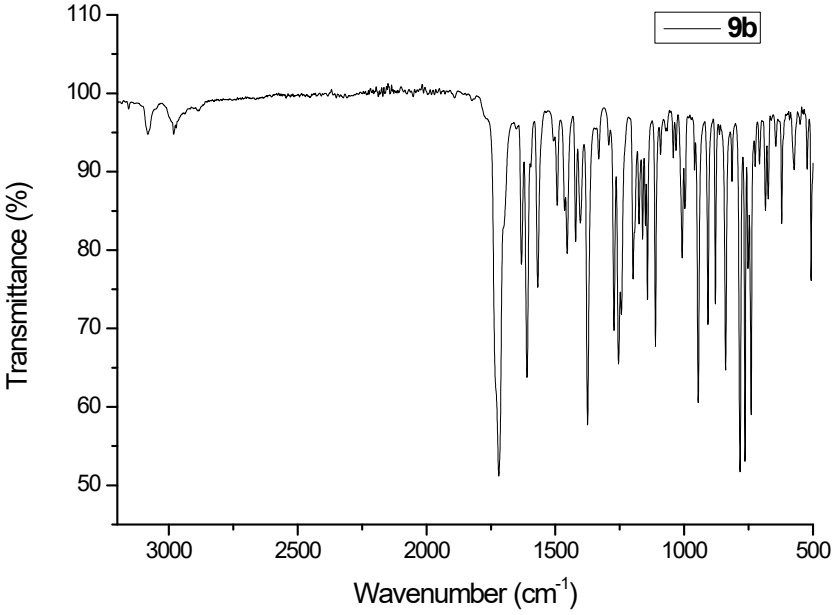

Figure S24. FTIR spectrum of **9b**.

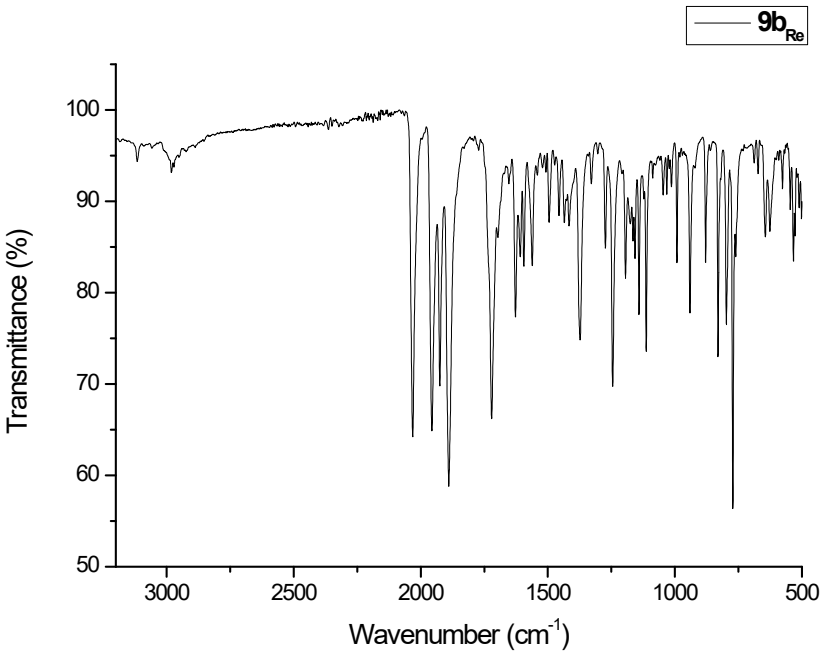

Figure S25. FTIR spectrum of **9b$_{Re}$.**

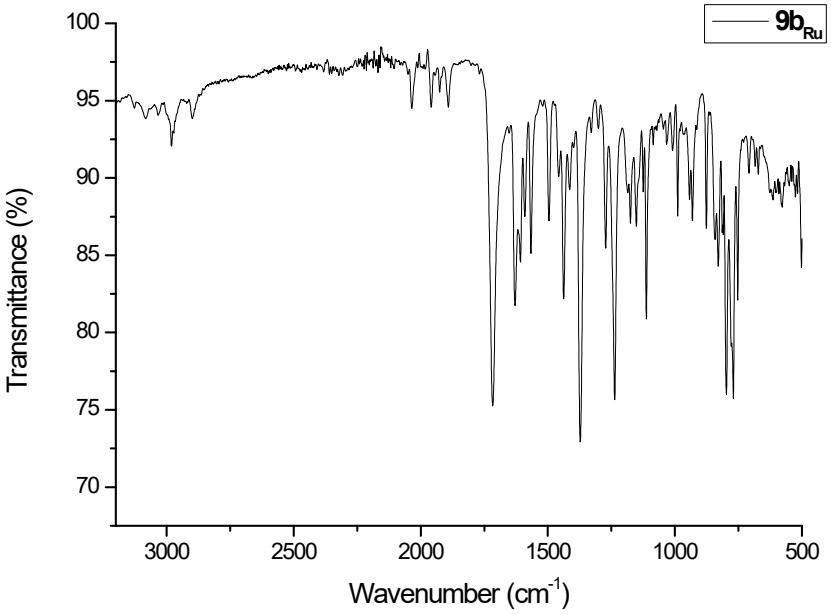

Figure S26. FTIR spectrum of **9b$_{Ru}$.**

3. UV-Vis spectra of ligands (7b, 9b) and complexes ($7b_{Re}$, $7b_{Ru}$, $9b_{Re}$, $9b_{Ru}$)

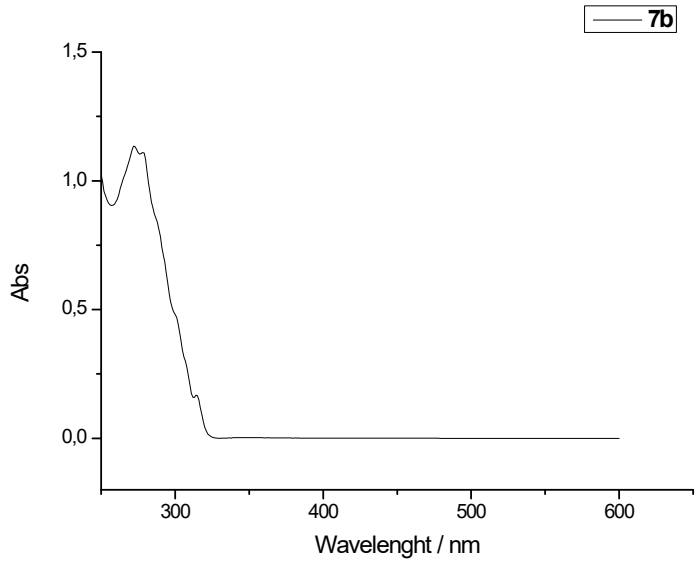

Figure S27. Absorption spectrum of derivative **7b** (c (ACN) = 10^{-4}).

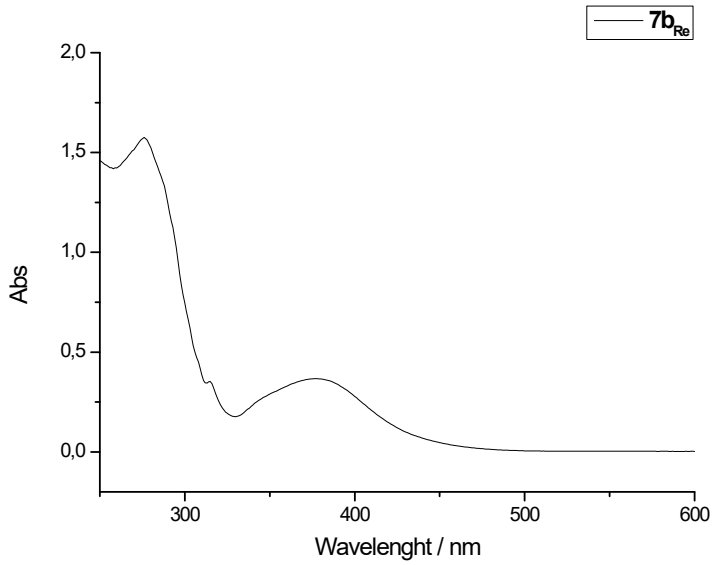

Figure S28. Absorption spectrum of derivative **$7b_{Re}$** (c (ACN) = 10^{-4} mol/dm^3).

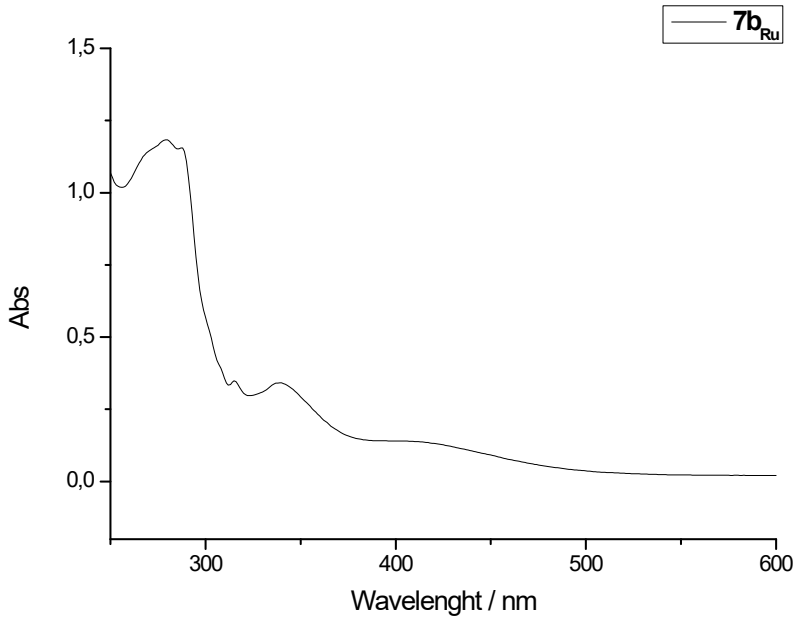

Figure S29. Absorption spectrum of derivative **7b$_{Ru}$** (c (ACN) = 10^{-4} mol/dm^3).

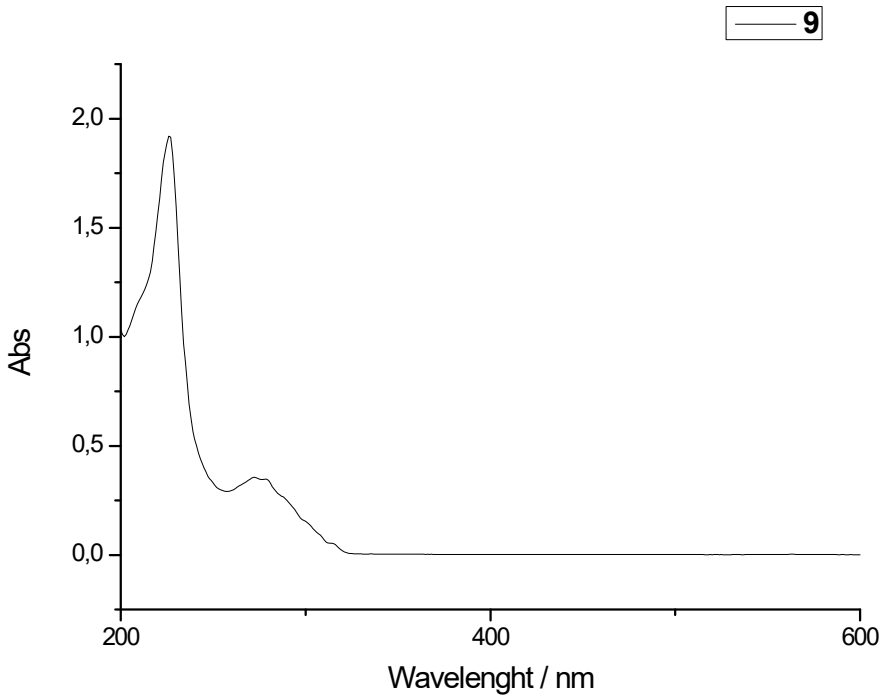

Figure S30. Absorption spectrum of derivative **9** (c (ACN) = 10^{-4} mol/dm^3).

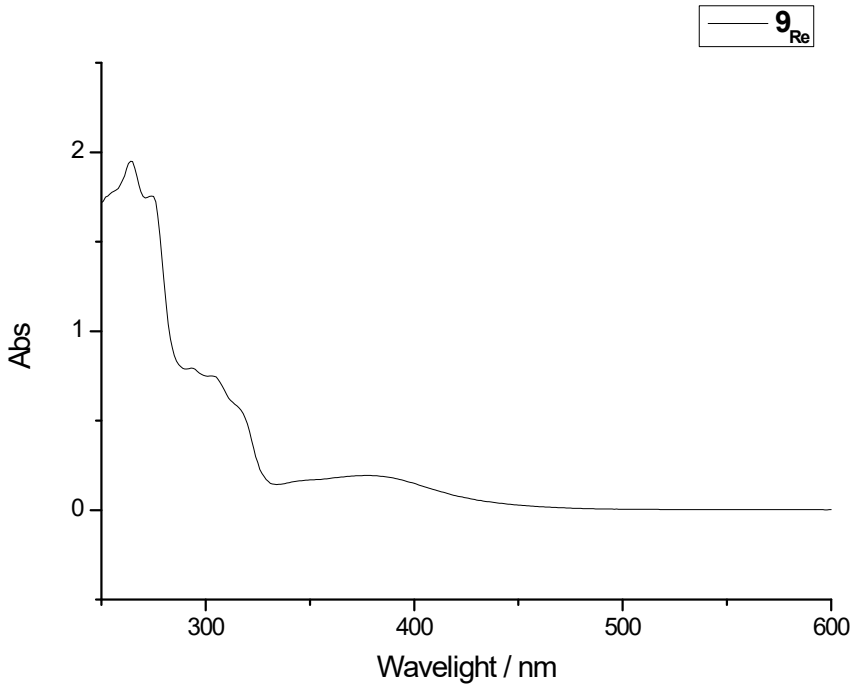

Figure S31. Absorption spectrum of derivative $\mathbf{9_{Re}}$ (c (ACN) = 10^{-4} mol/dm^3)..

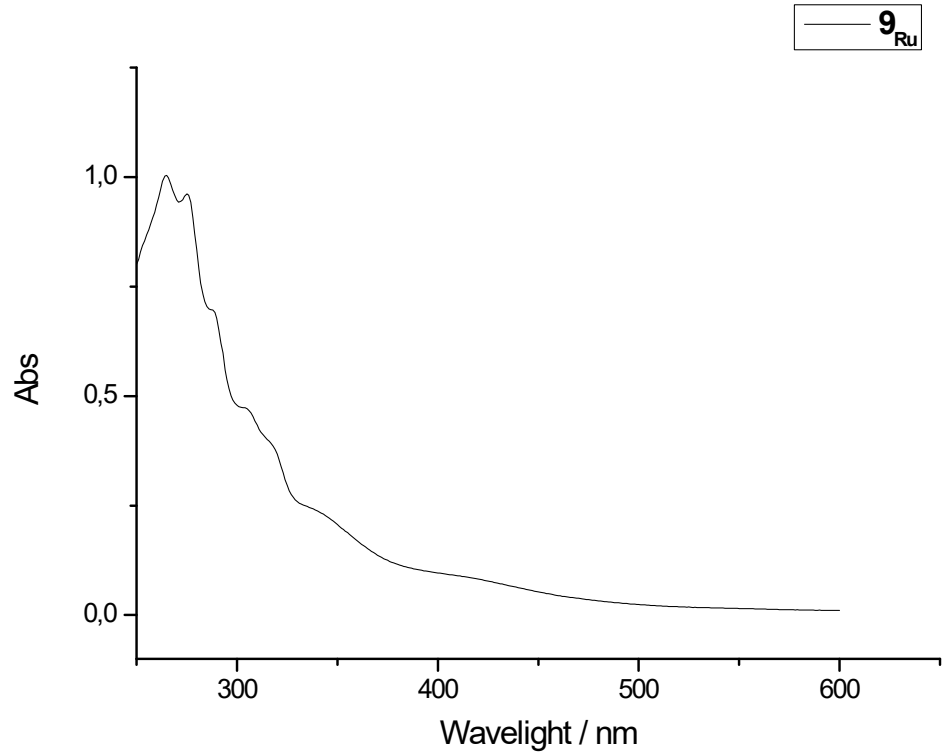

Figure S32. Absorption spectrum of derivative $\mathbf{9_{Ru}}$ (c (ACN) = 10^{-4} mol/dm^3)..

4. Molecular Docking Studies with Bcl-2

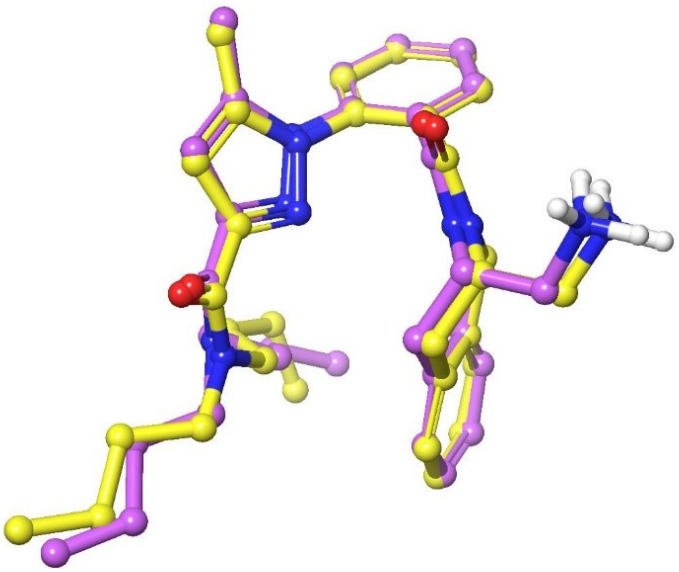

Figure S33. Comparison between the docked pose of the Bcl-2 inhibitor J1Q produced by the docking study (yellow) and the original crystallographic structure of the same inhibitor within the Bcl-2 binding pocket (Purple, PDB: 6QGK).

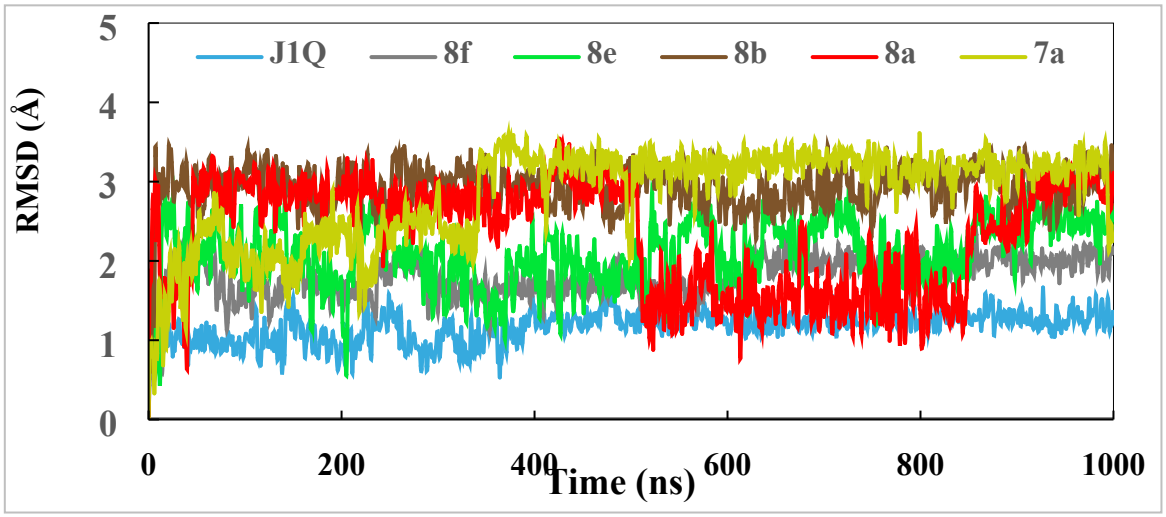

Figure 34. The RMSD of the backbone of Bcl-2 and complexes during the simulation period.

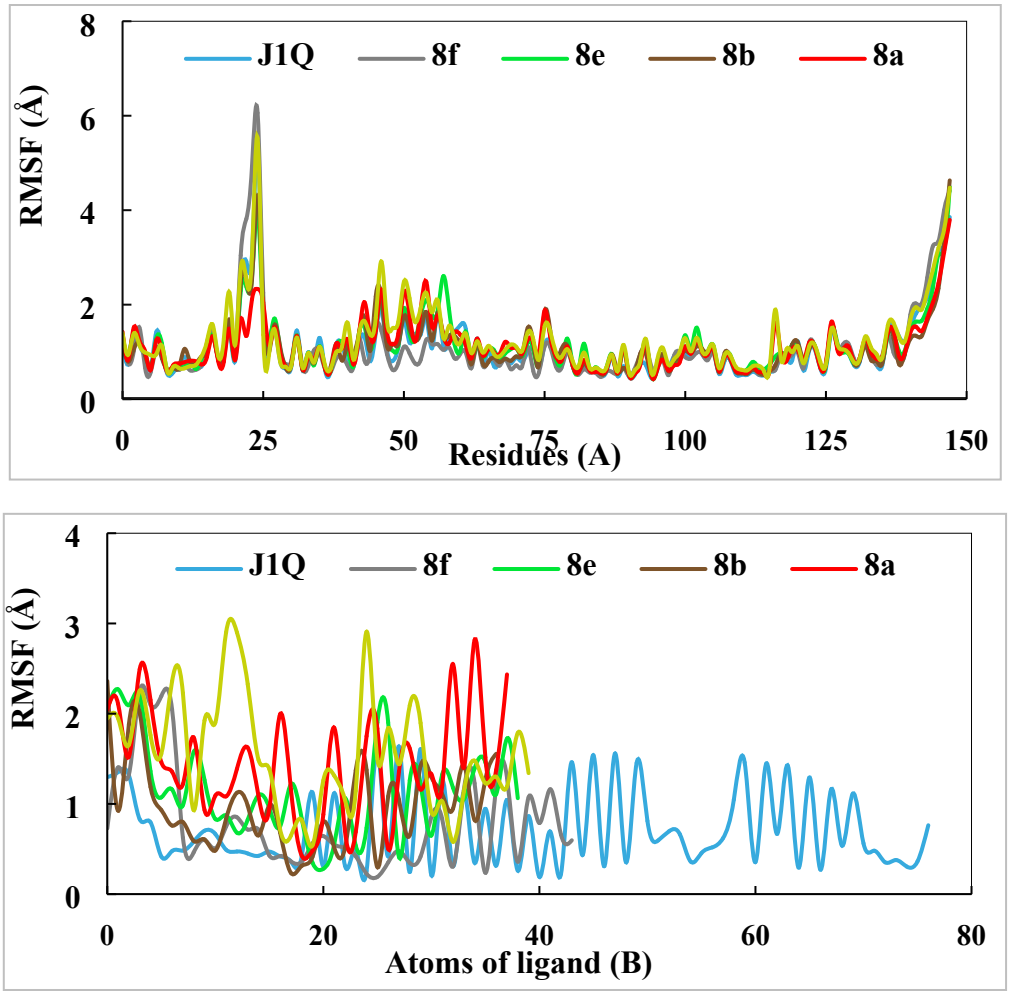

Figure 35. (A) The RMSF of Cα atoms of Bcl-2 in the absence and presence of ligands. (B) The average RMSF value of each atom of the ligands during MD simulation.

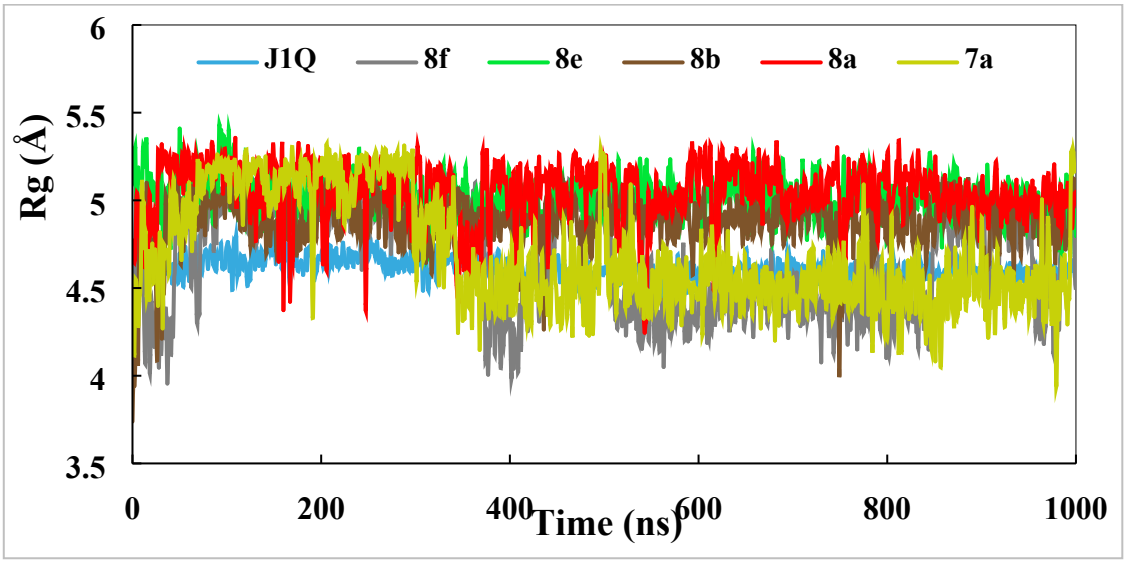

Figure S36. Radius gyration of the backbone of Bcl-2 and complexes during simulation.

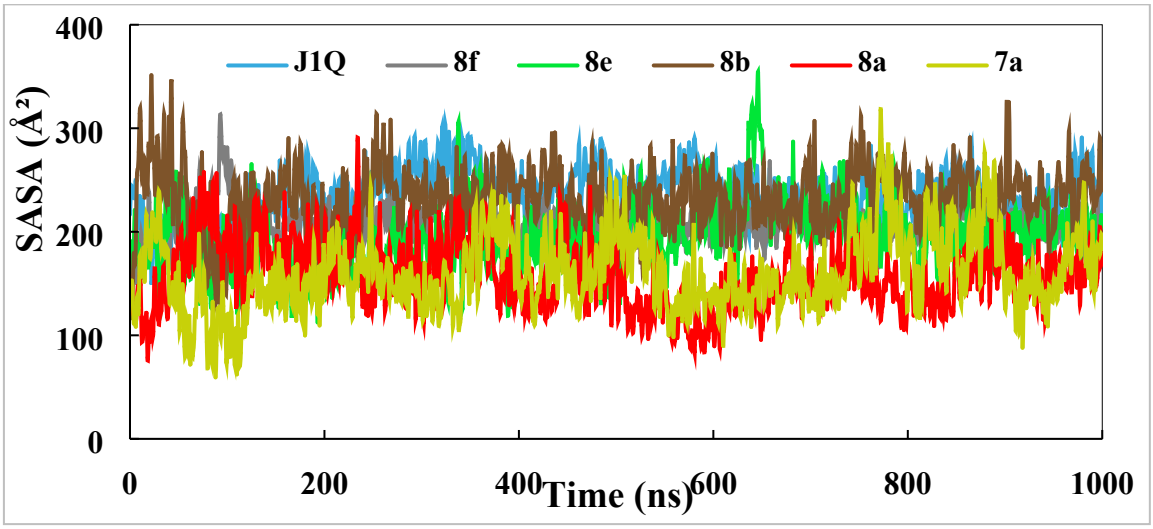

Figure S37. Solvent accessible surface area (SASA) of Bcl-2 and complexes during simulation.

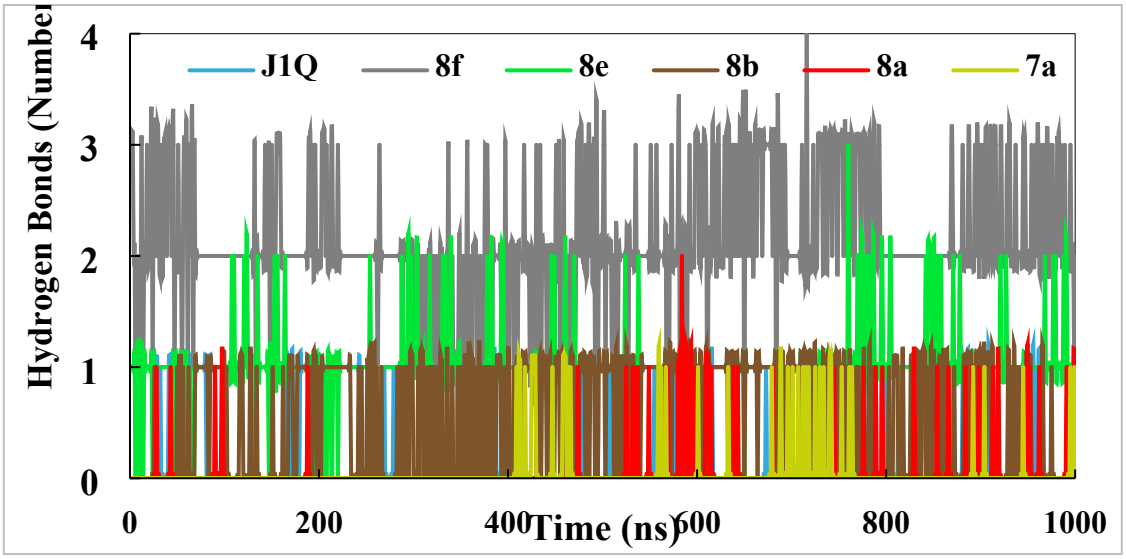

Figure S38. Number of hydrogen bonds between ligands and Bcl-2 during the simulation.